Available online at www.sciencedirect.com
SCIENCE DIRECT®
Progress in Oceanography 66 (2005) 89–119
Progress in Oceanography
www.elsevier.com/locate/pocean

General patterns of circulation, sediment fluxes and ecology of the Palamós (La Fonera) submarine canyon, northwestern Mediterranean

Albert Palanques [a,*], Emilio García-Ladona [a], Damià Gomis [b], Jacobo Martín [a], Marta Marcos [b], Ananda Pascual [b], Pere Puig [a], Josep-Maria Gili [a], Mikhail Emelianov [a], Sebastià Monserrat [b], Jorge Guillén [a], Joaquín Tintoré [b], Mariona Segura [a], Antoni Jordi [b], Simón Ruiz [b], Gotzon Basterretxea [b], Jordi Font [a], Dolors Blasco [a], Francesc Pagès [a]

[a] *Institut de Ciències del Mar (CSIC), Passeig Marítim de la Barceloneta 37-49, Barcelona 08003, Spain*
[b] *Institut Mediterrani d'Estudis Avançats (CSIC-UIB), C/Miquel Marquès, 21 E-07190 Esporles, Mallorca, Spain*

Received 5 July 2002; received in revised from 14 April 2003; accepted 29 July 2004
Available online 8 June 2005

Abstract

Currents, particle fluxes and ecology were studied in the Palamós submarine canyon (also known as the Fonera canyon), located in the northwestern Mediterranean. Seven mooring arrays equipped with current meters and sediment traps were deployed along the main canyon axis, on the canyon walls and on the adjacent slope. Additionally, local and regional hydrographic cruises were carried out. Current data showed that mean near surface and mid-depth currents were oriented along the mean flow direction (NE–SW), although at 400 and 1200 m depth within the canyon current reversals were significant, indicating a more closed circulation inside the canyon. Mean near-bottom currents were constrained by the local bathymetry, especially at the canyon head. The most significant frequency at all levels was the inertial frequency. A second frequency of about three days, attributed to a topographic wave, was observed at all depths, suggesting that this wave was probably not trapped near the bottom. The current field observed during the most complete survey revealed a meandering pattern with cyclonic vorticity just upstream from and within the canyon. The associated vertical velocity ranged between 10 and 20 m/day and was constrained to the upper 300 m. This latter feature, together with other computations, suggests that during this survey the meander was not induced by the canyon but by some kind of instability of the mean flow.

In the canyon, suspended sediment concentration, downward particle fluxes, chlorophyll and particulate C and N were significantly higher up-canyon from about 1200 m depth than offshore, defining, along with the different

* Corresponding author. Tel.: +34 93 2309500; fax: +34 93 2309555.
E-mail address: albertp@icm.csic.es (A. Palanques).

0079-6611/$ - see front matter
doi:10.1016/j.pocean.2004.07.016

hydrodynamics, two canyon domains: one from the canyon head to about 1200 m depth more affected by the canyon confinement and the other deeper than 1200 m depth more controlled by the mean flow and the shelf-slope front. The higher near-bottom downward total mass fluxes were recorded in the canyon axis at 1200 m depth along with sharp turbidity increases and are related to sediment gravity flows. During the deployment period, the increase in downward particle fluxes occurred by mid-November, when a severe storm took place. On the canyon walls at 1200 m depth, suspended sediment concentrations, downward particle fluxes, chlorophyll and particulate C and N were higher on the southern wall than on the northern wall inversely to the current's energy. This could be caused by an upward water supply on the southern canyon wall and/or the mean flow interacting with the canyon bathymetry. In the swimmers collected by the sediment traps, the dominant species was an elasipod holothurian, which has not been recorded in other canyons or elsewhere in the Mediterranean, indicating particular speciation.

Keywords: Submarine canyons; Water circulation; Sediment dynamics; Suspended particulate matter; Ecology; Sediment fluxes; North western Mediterranean Sea; Spain; Catalonia; Palamós Canyon

1. Introduction

Submarine canyons act as preferential conduits for the transfer of matter and energy, playing an important role in the exchange between the continental shelf and deeper zones (Drake & Gorsline, 1973; Durrieu de Madron, 1994; Gardner, 1989a; Hickey, Baker, & Kachel, 1986; Puig & Palanques, 1998a). However, their complex topography and the intense fishing activity carried out within their confines have represented quite serious obstacles interfering with detailed experimental studies. The result is a limited knowledge of the hydrodynamics, of the sources and mechanisms regulating fluxes of particulate matter (Gardner, 1989a, 1989b; Puig & Palanques, 1998a, 1998b) and of the biodiversity existing within canyon habitats (Gili, Bouillon, Pagès, Palanques, & Puig, 1999).

The hydrodynamics in submarine canyons basically depends upon several forcing conditions in the region such as general circulation, bottom morphology and atmospheric regime. Forcing conditions differ among canyons and can give different responses. Furthermore, the circulation within canyons is highly heterogeneous both along and across the canyons (Ardhuin, Pinot, & Tintoré, 1999; Hickey, 1995; Klinck, 1996). The canyon size relative to the internal Rossby radius of incident flow and the flow incidence pattern will determine the circulation regime and variability in the canyon (Alvarez, Tintoré, & Sabatés, 1996; Klinck, 1996). Conversely, the role played by atmospheric forcing is poorly known. Driving winds can cause intensification of upwelling in canyons, resulting in high vertical velocity of up to 80 m/day driven by such processes (Hickey, 1997). Additionally, low-frequency oscillations have been observed in bottom currents flowing along the axis of several canyons. In the Foix canyon, located off Barcelona (NW Mediterranean), these oscillations have been associated with up-canyon/down-canyon current reversals, which have in turn been related to variations in atmospheric pressure (Puig, Palanques, Guillén, & García-Ladona, 2000). Bottom current reversals of this type have also been observed in other canyons, but associated with other processes such as internal tides (Hotchkiss & Wunsch, 1982; Hunkins, 1988; Shepard, Marshall, McLoughlin, & Sullivan, 1979), with much higher frequencies than those reported for the Foix canyon. The effect of such processes on the canyon habitat ecosystem is poorly known (Hickey, 1995).

Within canyons, the hydrodynamic pattern may lead to the retention and/or re-suspension of particulate matter (Gardner, 1989a; Puig & Palanques, 1998a; Puig et al., 2000). Particulate matter transferred from the shelf through submarine canyons comes directly from continental runoff and/or re-suspension (e.g., during storms) and coastal biological productivity (Boyd & Newton, 1999; Thunell, 1998). However, although it is known that such transfers are conditioned by particulate matter inputs, topography and hydrodynamics outside and inside the canyon, the details of how the transfer events take place have not been sufficiently elucidated.

The flux of organic particulate matter is one of the least understood transport processes in the canyons. Submarine canyons incising the continental margin are the deep-sea habitats with the greatest accumulation of organic inputs from both the water column and the shelf (Buscail & Germain, 1997; McHugh, Ryan, & Hecker, 1992). Channelling of the lateral transport of matter from the shelf to deeper zones through submarine canyons gives rise to high biomass levels and planktonic (Greene, Wiebe, Burczynski, & Youngbluth, 1992) and benthic (Vetter, 1994, 1995; Vetter & Dayton, 1998) production rates. In addition, submarine canyons receive inputs of particulate matter through the vertical flux of the detritus of planktonic organisms inhabiting the water column.

Submarine canyons may constitute one of the pools of greatest diversity and highest production in the Mediterranean Sea. If so, they would play an important role in processes related to the transfer of matter and energy in a sea which, as an oligotrophic system overall, must have mechanisms for the efficient recycling of energy at different scales (Margalef, 1997). On the one hand, environmental, physical, and sedimentary heterogeneity should be reflected in spatial heterogeneity in the distribution of biological communities, be they microbial, planktonic or benthic. On the other hand, channelling of a high proportion of fluxes of matter from the continental shelf and slope through the canyons should result in high production levels, a factor which may in part account for the high concentrations of macrofauna recorded in certain canyons in the region (Cartes, 1998; Demestre & Martín, 1993; Stefanescu, Morales-Nin, & Massutí, 1994).

The Catalonian continental margin in the northwestern Mediterranean Sea (Fig. 1) is well suited for a detailed analysis of such processes, because several submarine canyons incise it. The main characteristics of the regional circulation pattern in this margin is a slope current referred to as the Northern current (Millot,

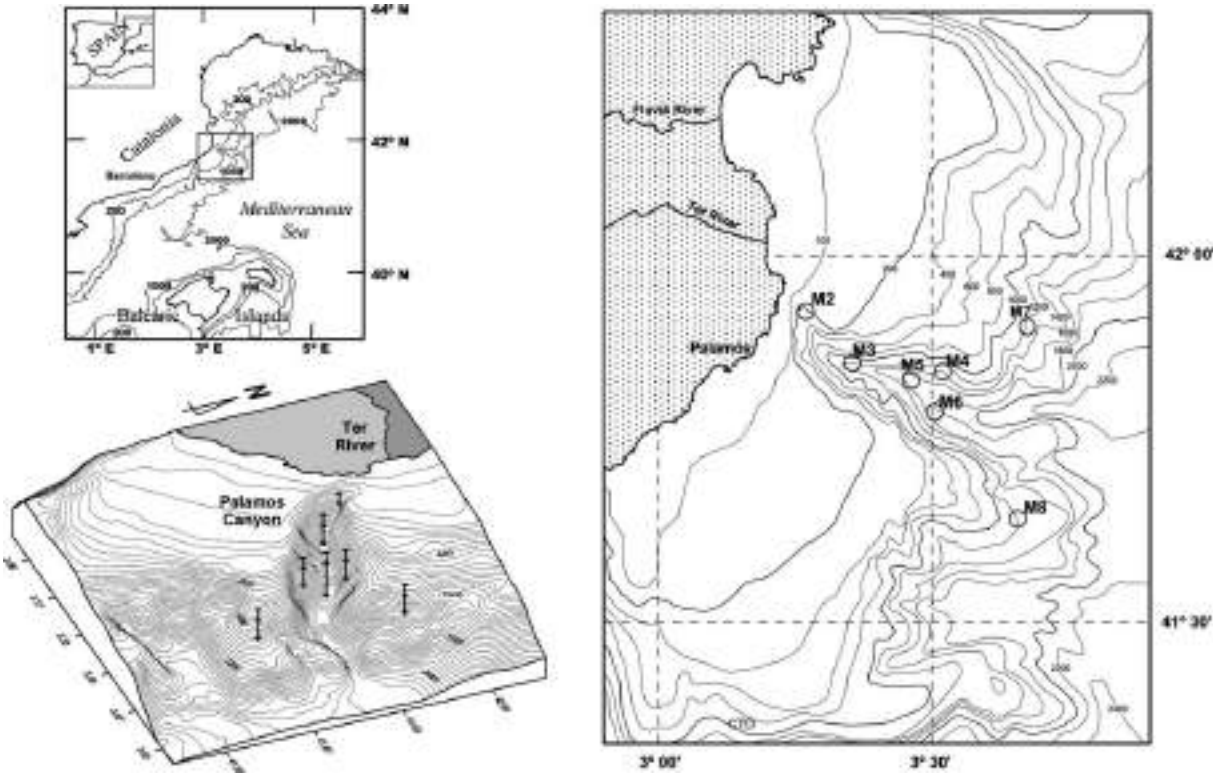

Fig. 1. General map of the study area, block diagram of the Palamós canyon showing moorings distribution and location map of mooring arrays.

1999), associated with a shelf-slope density front (Font, Salat, & Tintoré, 1988). This baroclinic current separates continental fresh waters from denser open sea saline waters (Castellón, Font, & García, 1990; García, Tintoré, Pinot, Font, & Manríquez, 1994). The circulation exhibits a seasonal variability with significant spatial mesoscale variability (Font, García-Ladona, & Górriz, 1995; La Violette, Tintoré, & Font, 1990; López García, Millot, Font, & García-Ladona, 1994), which plays a decisive role in exchange processes between shelf and oceanic waters (Tintoré, Wang, & La Violette, 1990; Wang, Vieira, Salat, Tintoré, & La Violette, 1988). The absence of significant tidal motions and of a prevailing wind field contributing to generalised upwelling enables one to focus on the internal dynamics of the currents and its interaction with topography as a permanent source of variability in the area (Alvarez et al., 1996; Masó & Tintoré, 1991). Due to these dynamical characteristics this region is a suitable place to analyse in detail the influence of canyon topography on the incident flow. The Palamós canyon (Fig. 1) (also known as the Fonera canyon) was selected because it is incised in the continental shelf and receives direct transfers of sediment inputs from the coastal zone and nearby rivers, such as the Ter River.

The purpose of this paper is to study a canyon system and to integrate results from: (1) the hydrodynamic pattern and associated physical processes, (2) the water turbidity and downward particle fluxes, (3) the seston biomass, and (4) the accumulation and speciation of planktonic and benthic species in the system.

2. Methods

The observational work consisted of a series of field measurements carried out from March to November 2001. Moored instruments and hydrographic surveys were combined, the latter including water sampling for biogeochemical analysis in the laboratory. The study of temporal variability was supplemented by time series analysis of satellite images (NOAA infrared) to monitor trends in the surface structure and seasonal sea and weather conditions.

2.1. Moored instruments

Mooring lines (Fig. 1) were equipped to collect time series of water currents, downward particulate matter, temperature, conductivity and water turbidity. Data were recorded by seven moorings with a total of 18 current meters and seven sediment traps deployed inside and in the vicinity of the canyon, near the sea bed and at intermediate levels (150 and 400 m depth) in the water column. Three moorings (M2, M3 and M5) were deployed along the canyon axis at depths of around 470, 1200 and 1700 m. Another two moorings (M4 and M6) were placed at the canyon walls at a depth of around 1200 m. The other two moorings (M7 and M8) were deployed at a distance of around 15 km upstream and downstream from the axis of the canyon, in order to monitor flow rates on the slope before and after the topographical perturbation represented by the canyon (Fig. 1). The mooring deployment period was divided into two parts for maintenance operations. Both the geographical location of the moorings and the vertical position of each instrument before and after the maintenance break were very similar. Differences between the bottom depths of the moorings after re-deployment were less than 50 m except in the case of mooring M8, which was re-deployed 135 m deeper (Table 1).

Each mooring was equipped with a current meter, a turbidimeter and a sediment trap near the bottom ($\sim$ 25 m above bottom) to collect data from the bottom nepheloid layer and to measure downward particle fluxes. The time sampling interval of the current meters was set to 30 min, with the exception of the near bottom instruments and the M2 and M3 moorings, for which it was set to 10 min. In order to remove the tidal components, the original current data set was subsampled at a 1-hour time interval and analysed by using the least squared fitting method. Sediment traps worked successfully throughout the deployment period. Sampling intervals of sediment traps were 9 days and 11 days for the first and second deployment respectively. A sketch with the available time series from the whole set of current meters is represented in Fig. 2.

Table 1
Mean currents measured by current meters for the two deployment periods

Mooring	Instr.	Depth (db)	$(\langle U\rangle, \langle V\rangle)$	$(\langle U\rangle, \langle V\rangle)$
M2	RCM-9	470–470	−0.06, 0.1	−0.2, 0.02
M3	RCM-9	110–149	−0.8, −3.4	−1.8, −3.2
	RCM-9	363–401	−0.3, 0.6	−0.02, 0.06
	RCM-9	1166–1206	−0.6, −0.10	−0.8, 0.4
M4	RCM-7	236–204	0.03, −0.8	0.06, −0.6
	RCM-7	500–475	−0.5, −1.9	0.3, −1.3
	RCM-9	1301–1299	−3.0, −7.7	−1.5, −6.0
M5	RCM-7	130–162	−3.5, −16.0	−1.4, −9.4
	RCM-9	1728–1747	−1.1, −0.01	0.7, 0.2
M6	RCM-9	1327–1281	0.02, −0.4	0.3, −0.3
M7	RCM-7	290–257	−1.7, −4.4	−1.5, −3.7
	RCM-7	530–490	−1.7, −2.3	−1.3, −0.9
	RCM-9	1310–1260	–	0.8, −0.4
M8	RCM-7	135–278	−3.2, −7.3	−0.5, −3.0
	RCM-7	380–525	−1.2, −2.9	−0.3, −2.0
	RCM-8	1164–1290	0.5, −1.7	0.7, 0.07

The values of the depth column correspond to pressure level of instruments for the first and second deployment periods respectively.

2.2. Oceanographic cruises

Four oceanographic surveys were carried out in the study area. The most intensive survey was CANYONS II, carried out between 24 and 31 May 2001. A domain of $80 \times 70\ km^2$ was covered by 134 CTD stations 4 km apart just over the canyon (a subdomain of $25 \times 40\ km^2$) and 8 km elsewhere (Fig. 3B). The other cruises repeated the stations transect along the axis and two station transects across the canyon (Fig. 3A). At each station CTD vertical profiles including fluorescence and turbidity were recorded and water samples were collected using a rosette of Niskin bottles for conventional chemical and biological analyses (nutrients, standard chlorophyll, and primary productivity) at different levels. Direct velocity measurements were collected using a 153.6 kHz Vessel-Mounted Acoustic Doppler Current Profiler (VM-ADCP). The vertical resolution was configured to 8 m and the sampling period to 2 min. After calibration and correction of errors induced by ship motion, individual profiles were averaged into 10-min ensembles. CTD transects were represented using the ''Ocean Data View'' (Schlitzer, 2003).

2.3. Processing of hydrographic data

The hydrographic variables measured on the CANYONS II cruise were interpolated from station points onto grid points using a successive correction scheme with weights normalised in the observation space in order to approach Optimum Statistical Interpolation (Bratseth, 1986). The horizontal characteristic scale of the spatial interpolation was set to 15 km, according to correlation statistics. An additional normal-error filter convolution was also applied in the way proposed by Pedder (1993) in order to filter out scales that cannot be resolved by the sampling. The cut-off wavelength was set to 15 km. Dynamic height (the vertical integration of specific volume anomaly) was computed from station T, S profiles and referred to 600 m, which is a usual reference level in the basin (e.g., Pinot, Tintoré, & Gomis, 1995). Derived dynamical variables such as geostrophic velocity or geostrophic vorticity were then obtained by finite-differences from interpolated grid point values of dynamic height. Vertical velocities were derived by integrating the Q-vector form

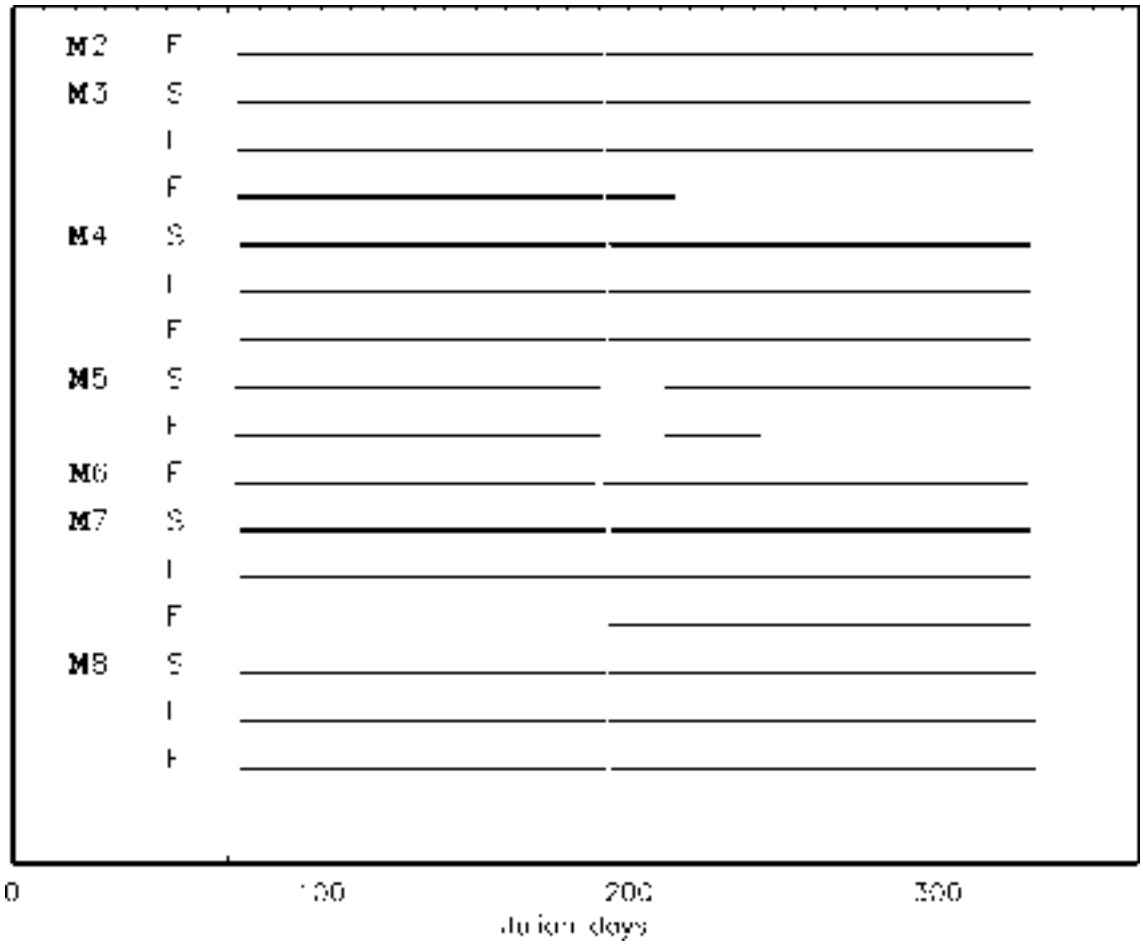

Fig. 2. Time diagram of the available time series for each current meter of every mooring in near-surface (S), near-bottom (F) and mid-water (I) depths. Sediment traps and the moored ADCP worked successfully during all the deployment period.

of the Quasi-Geostrophic (QG) omega equation (Hoskins, Draghici, & Davis, 1978). This was integrated by setting $w = 0$ at the upper and lower boundaries and setting its normal derivative to zero at the lateral boundaries (for a detailed description of the method, see Pinot, Tintoré, & Wang, 1996).

2.4. Laboratory analysis

Sediment trap samples were processed in the laboratory for subsampling and to estimate the total mass flux according to the method described by Heussner, Ratti, and Carbonne (1990). Carbon and Nitrogen content of the sediment trap samples was analysed using a CN 2000 LECO analyser. Opal content was analysed following the method of Mortlock and Froelich (1989). The swimming organisms captured by the sediment traps were studied to species level and compared with the previous studies carried out in three other northwestern Mediterranean canyons (Gili et al., 2000). Current meters data were calibrated and processed following standard procedures for their interpretation. Turbidimeter data collected in FTU were converted into suspended sediment concentration following the methods described in Guillén, Palanques, Puig, Durrieu de Madron, and Nyffeler (2000).

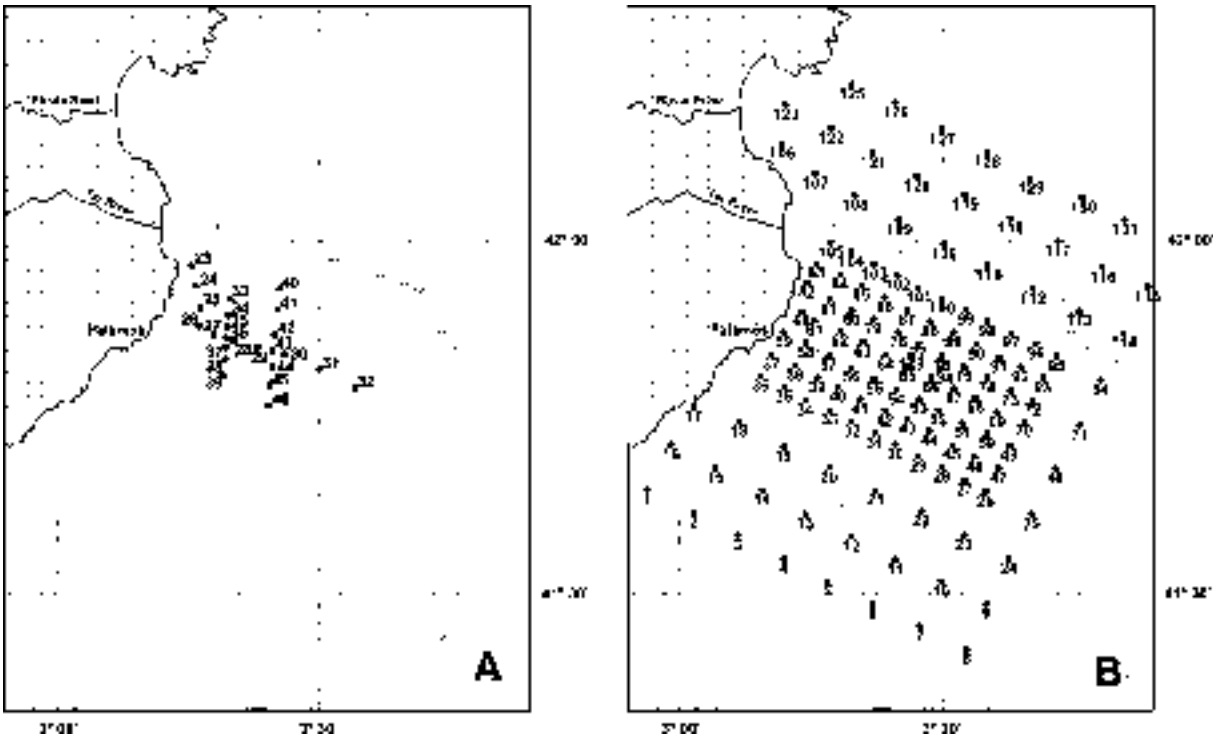

Fig. 3. Location map of (A) CTD stations during cruises CANYONS I (March 2001), III (July 2001) and IV (November 2001). (B) CTD stations during CANYONS II cruise (May 2001).

For the analysis of the total particulate carbon (TPC) (including both organic and inorganic carbon) and nitrogen (TPN) content in the water samples, three 800-ml replicates were filtered through precombusted (450 °C, 5 h) GF/F filters and immediately frozen in liquid nitrogen. Subsequently, the filters were dried at 60 °C for 24 h. The samples were analysed using a CN autoanalyser (Perkin-Elmer 240).

Chlorophyll concentrations were measured at the pigment laboratory of the ICM by fluorometry (Yentsch & Menzel, 1963). From each depth, 100 ml of water were filtered through Whatman GF/F glass fibre filters (25 mm diameter) for total chlorophyll estimation. The filtrations were done at low vacuum pressure (< 100 mmHg). After the filtration the GF/F filters were frozen immediately at −70 °C. The filters were subsequently placed in 6 ml of 90% acetone for approximately 24 h in the dark and at 4 °C. The fluorescence of the extract was measured with a Turner-Design fluorometer. The chlorophyll values were used to calibrate the sensor of fluorescence of CTD MK-III, which gave a correlation of 0.8583.

3. Results

3.1. Time variability of currents recorded by moored instruments

To give a general overview of the current field, as measured by the moored current meters, scatter plots of the velocity components and the distribution of direction for the full sampling period are presented in Figs. 4–6 (note that data from the two sampling periods are merged) and the basic statistics is listed in Table 1.

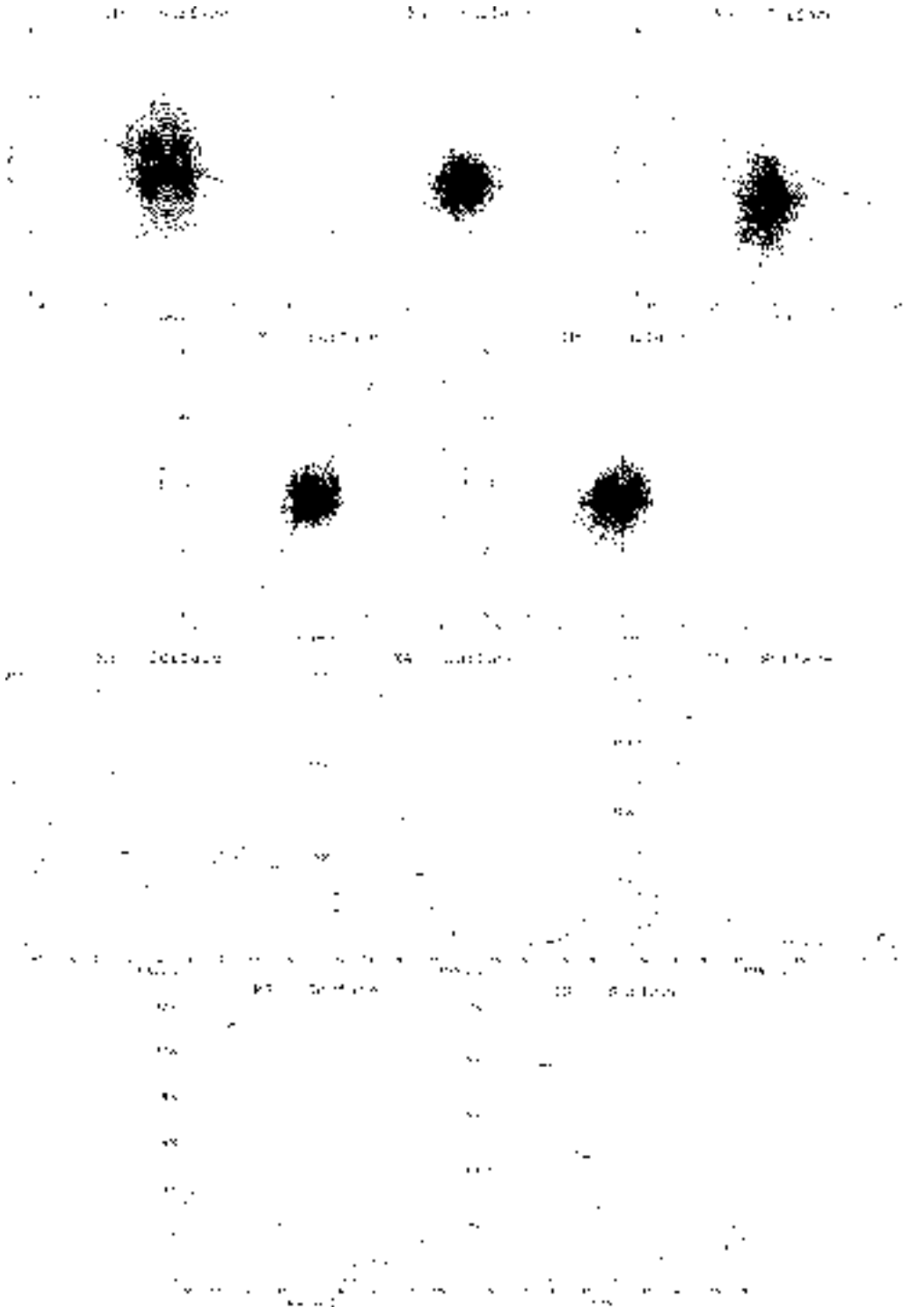

Fig. 4. Scatter plots and distribution of velocity directions for the full sampling period measured by the current meters installed at the upper levels. Directions are binned in intervals of 10°. The solid lines overdrawn represent the direction of the isobaths at the mooring site with both directions (alpha, pi-alpha).

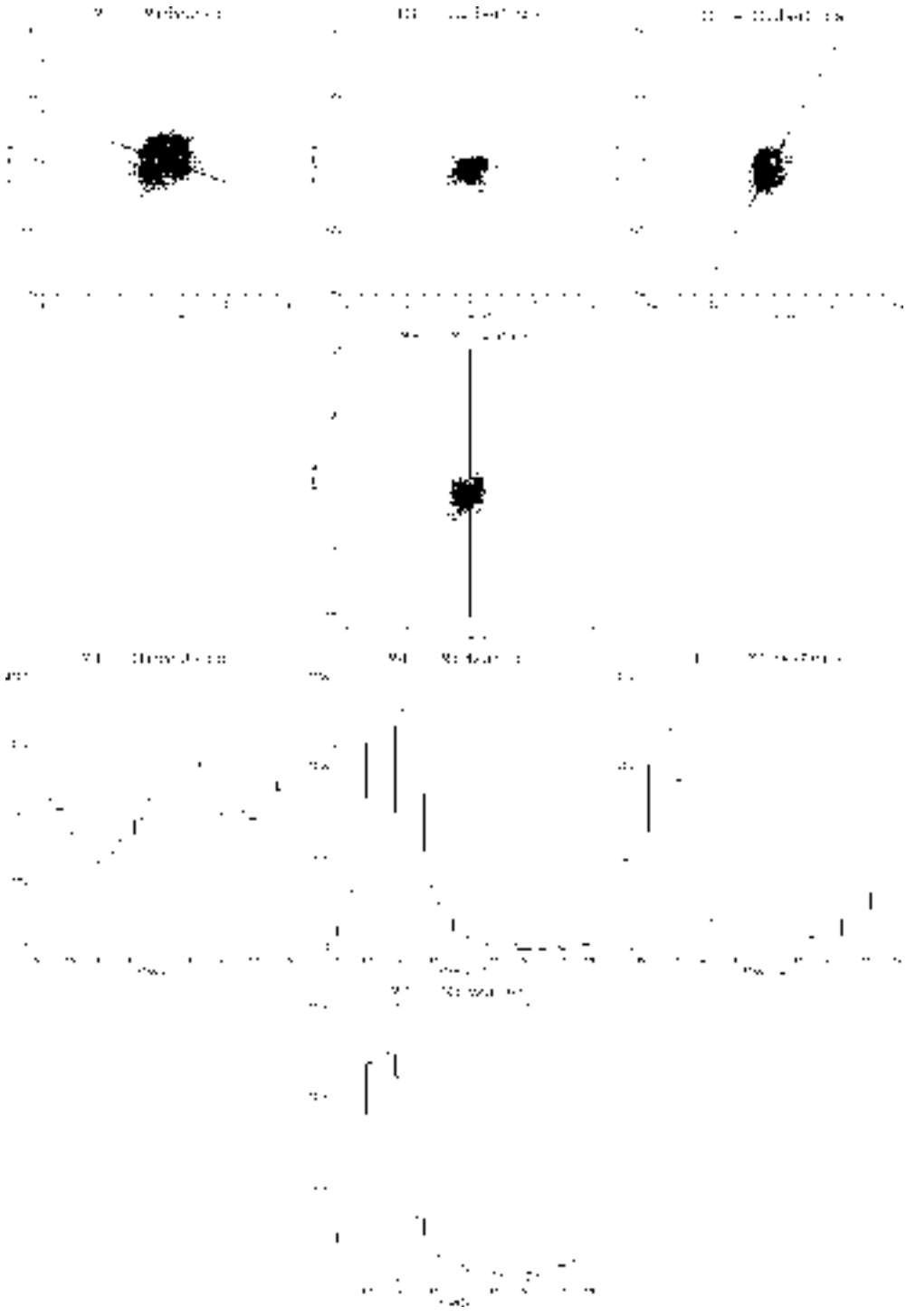

Fig. 5. Scatter plots and distribution of velocity directions for the full sampling period measured by the current meters installed at mid-water depths. Directions are binned in intervals of 10°. The solid lines overdrawn represent the direction of the isobaths at the mooring site with both directions (alpha, pi-alpha).

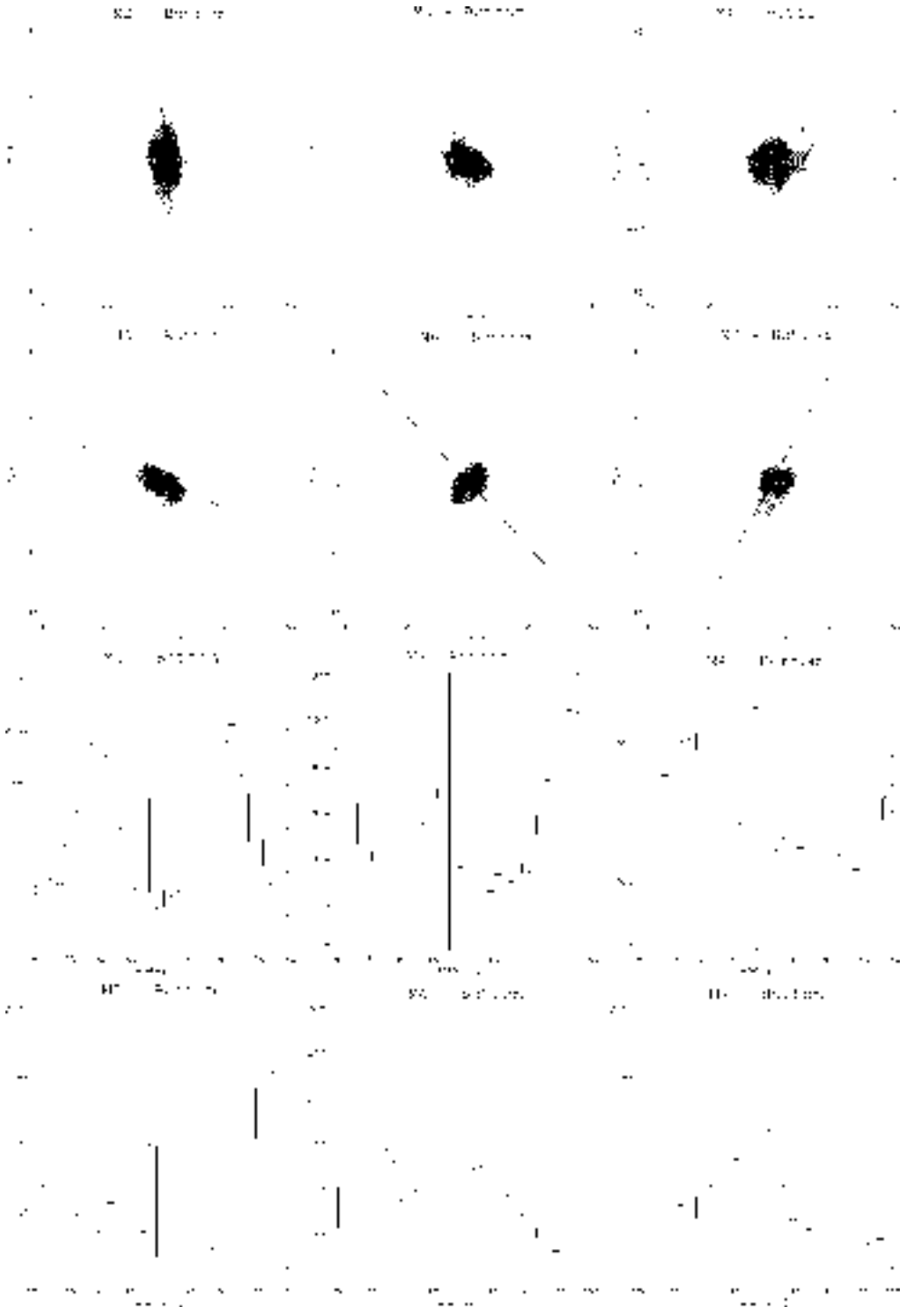

Fig. 6. Scatter plots and distribution of velocity directions for the full sampling period measured by the current meters installed near the bottom. Directions are binned in intervals of 10°. The solid lines overdrawn represent the direction of the isobaths at the mooring site with both directions (alpha, pi-alpha).

Near-surface currents exhibit the main characteristics of the regional circulation in the area: mean currents between 100 and 300 m water depths clearly along the mean direction (NE–SW) of the regional circulation driven by the shelf-slope density front (Fig. 4). Maximum mean currents are found in the mid-canyon area, mainly in the canyon axis (at M3 and particularly at M5), with maximum values of about 60 cm/s recorded at M5. The latter was expected to correspond to the mean location of the frontal jet dominating the local circulation. Near the canyon head and still over the axis (M3), mean near-surface currents are lower and more variable in direction (Fig. 4). The currents often exhibit reversals with respect to the predominant mean current direction, which have been observed to persist for several (4–6) days. Outside the canyon, on both the northern and southern walls, mean currents are still aligned with the frontal jet, and although their direction coincides with local isobath directions, this does not imply a topographic forcing.

At intermediate levels within the canyon, mean currents are of course lower than at upper levels, and flow directions are more isotropically distributed (M3 in Fig. 5). A noteworthy feature is the marked peak along the canyon axis direction in the mooring located at the head of the canyon. On the northern wall of the canyon, currents are still across isobaths, with a mean SW direction. Outside the canyon the flow is mainly along the slope, that is, following the mean flow direction as in the upper levels.

Near the bottom, mean currents are smaller, as expected, but maximum peaks are still around 15–20 cm/s for almost all instruments (Fig. 6) and even greater for M2, although this corresponds to a current meter located at a shallower depth (470 m) than the others (>1000 m). The currents within the canyon are more constrained by the local bathymetry and the canyon shape. This is particularly relevant near the canyon head in the canyon axis (mooring M2) where velocities are mainly oriented along the axis of the canyon, up and down with almost the same probability. Down-canyon along the axis (M3 and M5), the mean current directions are also parallel to the local bathymetry but they show a greater variability, which is more relevant in the case of M3 than M5. At the canyon walls (M4 and M6) currents are not clearly in the along-isobath direction. In fact, at M6 (southern wall), the cloud of scatter points is more elliptical and seems to be in the across-isobath direction. However, in both cases it is difficult to specify the relationship of currents with bathymetry because the local topography of the canyon walls could be highly variable, depending on small-scale unresolved morphological features such as gullies and scours. An interesting question is the clear asymmetry between the northern and the southern wall of the canyon. Though the mean current is very similar at both sites (Table 1), the instantaneous currents are slightly larger on the northern wall (M4) than on the southern wall (M6).

In order to analyse the temporal variability of the currents, the velocity components were rotated to have along-slope and cross-slope components. Spectral analysis of the current series shows that the most significant spectral peak for both current components at all levels is the inertial frequency, at 18.07 h (Fig. 7A). It appears sharply at surface levels but is also clear for bottom locations. Spectra of bottom current records at both canyons walls (M4 and M6) show the asymmetry stated above, with higher energy on the northern wall for the whole deployment over a wide range of frequencies (Fig. 7B). A second peak located at around 3 days is also clearly seen at bottom locations, but not well identified at upper levels due to the high energy content at low frequencies. This periodicity has been detected before in different locations along the continental shelf and has been identified as a topographic wave propagating south-westward along the shelf (Flexas, Durrieu de Madron, Garcia, Canals, & Arnau, 2002; Millot, 1985; Sammari, Millot, & Prieur, 1995). An EOF analysis of currents confirmed the presence of the 3-day peak also at upper levels, suggesting that this wave is probably not trapped near the bottom as previously suggested by other authors (Fig. 8).

3.2. Spatial variability of currents inferred from quasi-synoptic cruise data

A first overall view of the hydrodynamic conditions simultaneous to the oceanographic cruises can be inferred from AVHRR images. The images presented here correspond to May 27th 2001 and May 30th

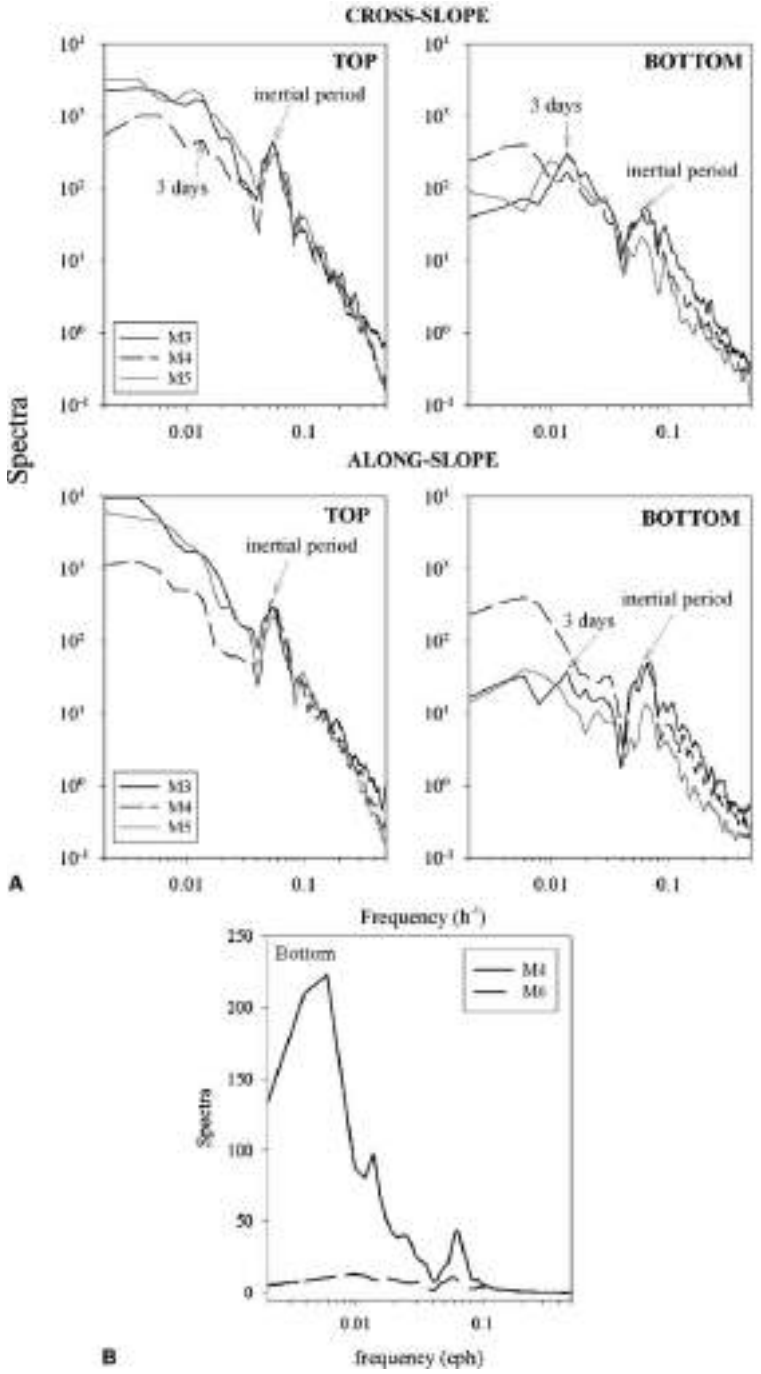

Fig. 7. (A) Spectra of along-canyon and cross-canyon components of current velocity for surface and bottom records at locations M3, M4 and M5. They were computed using a Kaiser-Bessel window with 256 points, resulting in 20 degrees of freedom. (B) Spectra of the along-canyon component at bottom depths for locations M4 (solid line) and M6 (dashed line). Analysis was carried out using a Kaiser-Bessel window with 512 points, resulting in 44 degrees of freedom.

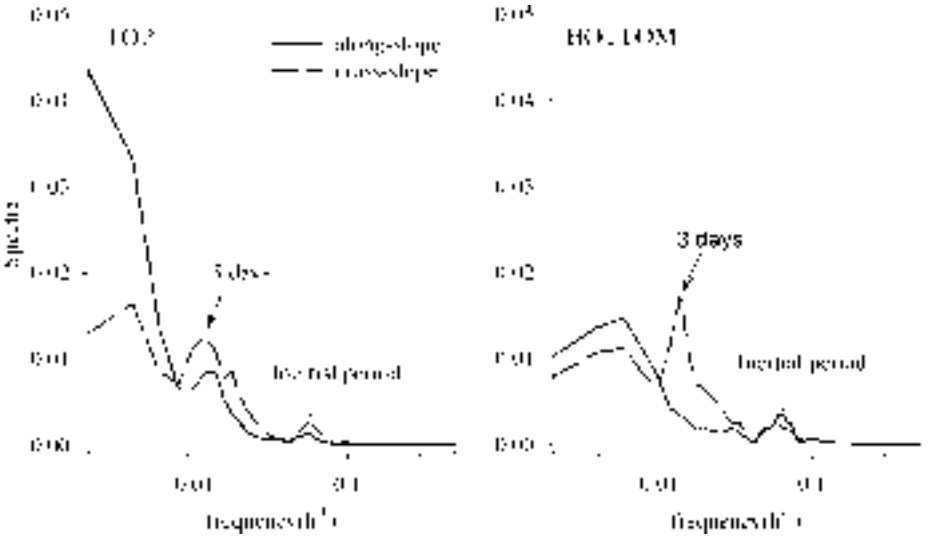

Fig. 8. Spectra of the first mode accounting for the 40% of the variance of the EOF analysis of currents for the top and bottom layers.

2001 (Fig. 9), i.e., they are simultaneous to the CANYONS II cruise. While on the 27th a thin cold meandering jet running along the coast can be identified with the thermal signature of the Northern current (Fig. 9A), on the 30th this feature is hidden by a strong warm signal which is probably due to the influence of the Rhone river runoff (Fig. 9B). The marked differences in the SST field suggest that the stationarity hypothesis assumed for most of the dynamical derivations (i.e., that the time scales of relevant features are much larger than the time taken to sample the domain) can be questioned at least at upper levels.

In agreement with the AVHRR image of May 30th, the most outstanding feature of the surface temperature field (i.e., at 10 m, Fig. 10A) is the presence of a tongue of warm water intruding the northern corner

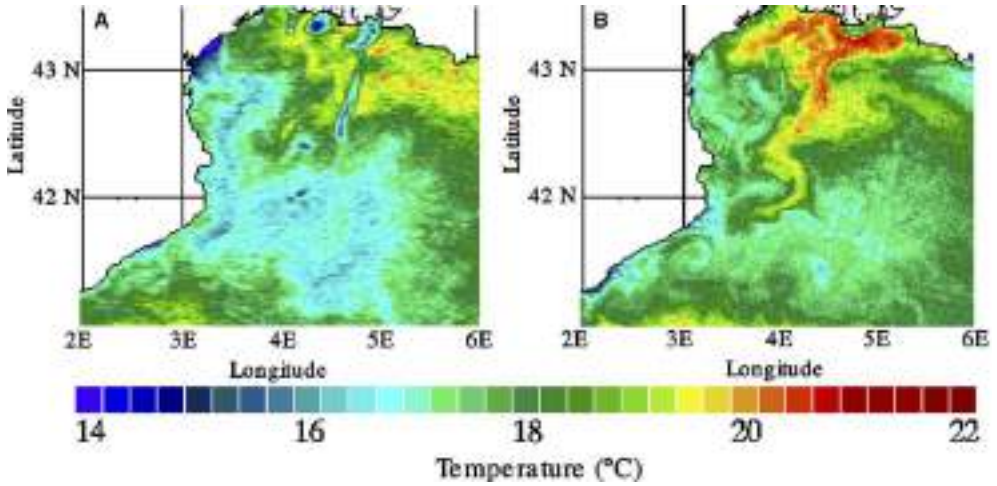

Fig. 9. AVHRR images of 27-May-2001 (A) and 30-May-2001 (B) (they were acquired and processed at IFA in Rome, Italy).

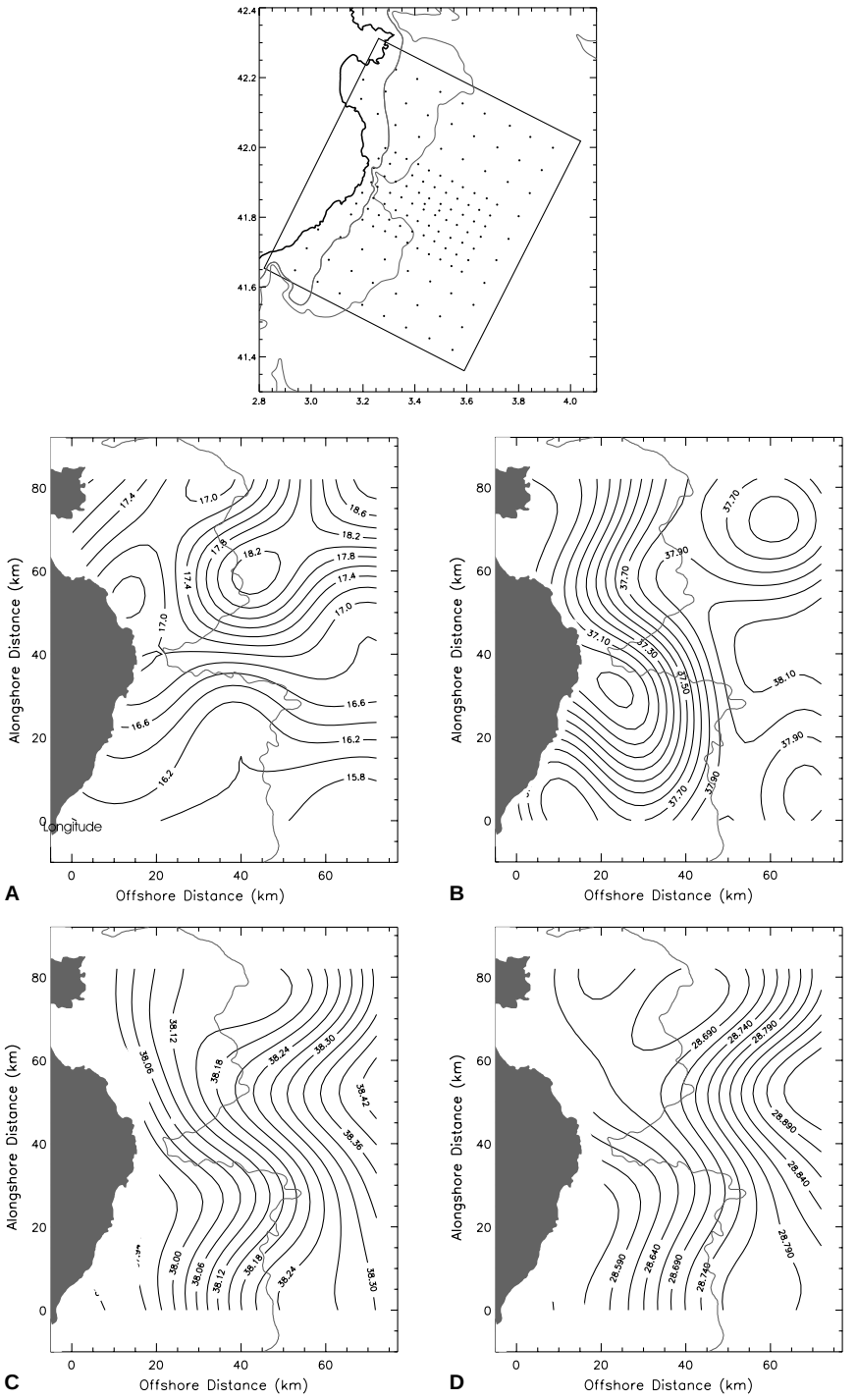

Fig. 10. Horizontal distribution at 10 m of (A) temperature (°C) and (B) salinity. Horizontal distribution at 100 m of (C) salinity and (D) density. The figures are rotated 27° in an anticlockwise sense and the axes do not coincide with latitude/longitude. The orientation of the grid is indicated in the upper map.

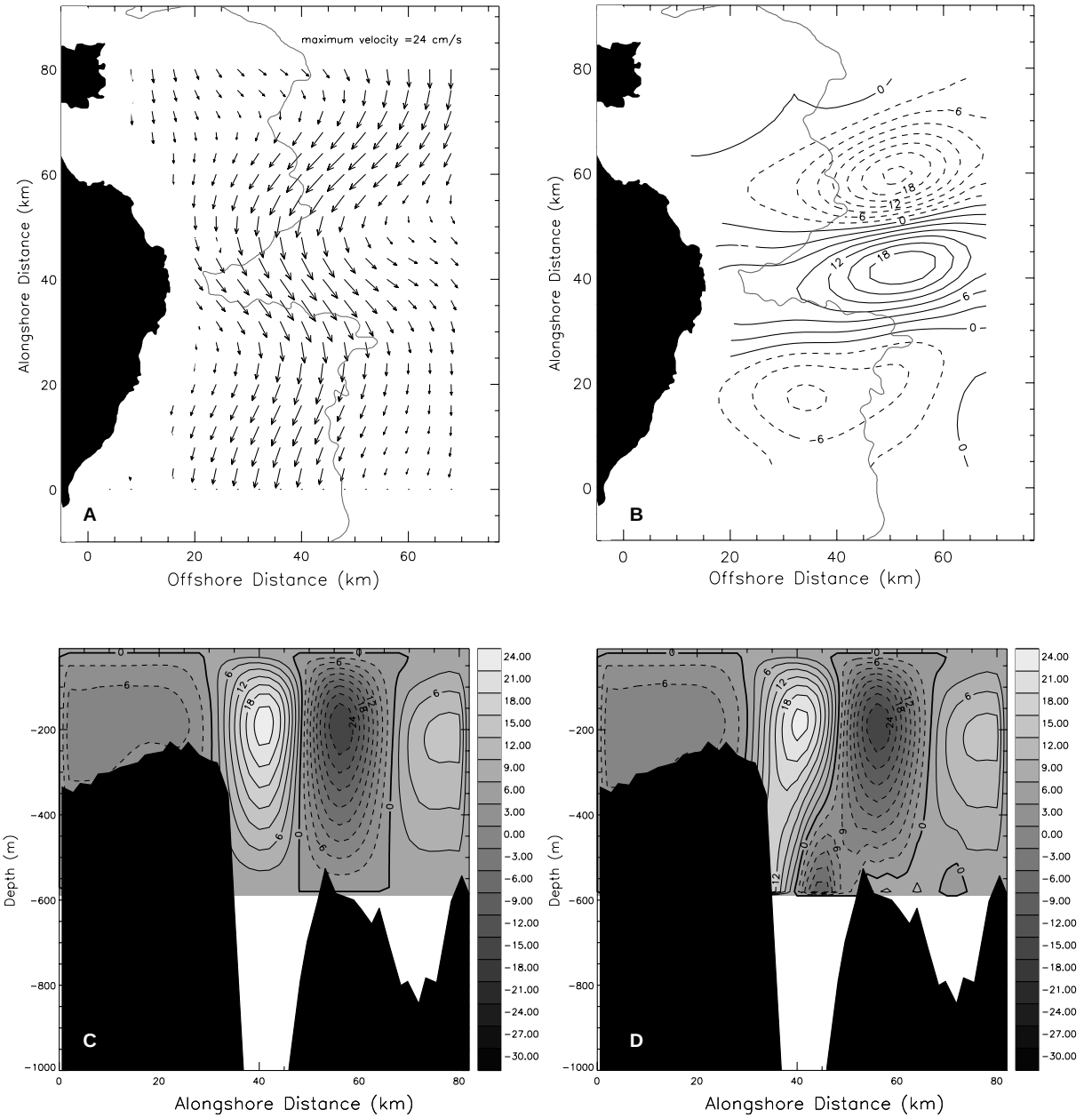

Fig. 11. (A) Geostrophic velocity at 100 m. Units are cm/s. (B) Vertical QG-velocity. Units are m/day and negative values (downward velocities) are dashed. (C) Vertical section perpendicular to the canyon axis showing the vertical velocity obtained from integrating the omega equation with $w_b = 0$ as lower boundary condition. The vertical section is located 40 km in the offshore direction, and the direction of the mean flow is from the right to left in the figure. (D) As in (C), but using $w_b = -v_{geostrb} \cdot \Delta h$ as the lower boundary condition.

of the domain (note that May 30th is the date on which CTD profiles were obtained at the northern boundary of the domain). The salinity values associated with this warm water (Fig. 10B) are about 37.6 and are not the lowest of the sampled domain. The surface salinity distribution shows a strong meandering

cross-shore gradient over the shelf, with fresher waters (<37.0) near the coast. The data of the Ter and Fluvià rivers runoff (not shown) confirm that there was a river discharge increase during the week of the cruise.

At 100 m, the salinity field is by far the dominant contribution to the density field (Fig. 10C) and therefore temperature is not shown. The distribution is characterised by the presence of a meandering salinity front, corresponding to the well-known shelf-slope front (the Catalan front; see e.g. Font et al., 1988) separating coastal fresher waters from the denser waters offshore.

The geostrophic current associated with the shelf-slope front (the Northern current) is clearly apparent flowing to the Southwest (Fig. 11A). At the northern boundary of the domain the flow is deflected onshore, with a marked anticyclonic curvature, whereas just upstream from and within the canyon it describes a cyclonic meander. Finally, downstream of the canyon, the flow veers again towards the coast with weak anticyclonic vorticity. The meander has an apparent wavelength of about 50 km, amplitude of about 20 km and maximum velocities at 100 m of about 24 cm/s.

The vertical velocity field (Fig. 11B) is consistent with the described meandering pattern, with maximum downward (upward) velocities obtained where anticyclonic (cyclonic) vorticity is advected by the mean flow (i.e., vertical motion is mainly a consequence of the vertical differential advection of relative vorticity by the mean flow). In our domain this means that downward motion is obtained before the upstream wall and after the downstream wall of the canyon, whereas upward velocities are obtained within the canyon. The maximum values of vertical velocities are about 18 m/day (both positive and negative). It is worth noting that the two strongest nucleus of vertical velocities are located offshore, where all CTD casts reached the reference level. This means that these cores are real since they are not associated with any artefact of the extrapolation of the dynamic height field near the coast. Conversely, the magnitude of vertical velocities is more uncertain due to the assumption of the reference level as a level of no motion and also due to errors involved in the interpolation procedure. At lower levels the 3D circulation pattern is about the same, although density gradients are obviously less marked and therefore the geostrophic current is smaller (not shown).

The described vertical velocity pattern was obtained by setting $w = 0$ as the lower boundary condition for the integration of the omega equation. This constraint could be critical in our case, since the submarine canyon could be forcing a significant up- or down-slope vertical motion and the vertical velocity at the deepest layer of our domain (600 m) could be substantially different from zero. To estimate this effect we also integrated the omega equation with the lower boundary condition of no flow through the canyon walls: $w_b = -v_{geostrb} \cdot \Delta h$, where h is the bathymetry depth, and $v_{geostrb}$ is the horizontal geostrophic velocity at the bottom of the domain.

Figs. 11C and D compare, on a vertical section perpendicular to the canyon axis, the vertical velocities obtained from integrating the equation with the two sets of lower boundary conditions. These figures reveal how the vertical velocity patterns due to the topography and to the meander are displaced relative to each one. The effect of the bottom topography is negligible above 300 m. These results support the hypothesis that the observed meandering pattern and the associated vertical velocity observed at upper levels is decoupled from the canyon topography. This is in agreement with current meter data, which showed no clear topographic forcing at upper levels.

The consistency of the 3D circulation obtained in the framework of quasi-geostrophic theory is supported by the good agreement between geostrophic and independent (VM-ADCP) velocity observations (Fig. 12). This by itself does not imply that the canyon does not significantly affect the circulation, but only that the overall mass field and the associated circulation are dominated by quasi-geostrophically balanced scales. This is confirmed by a simple scale analysis: taking the observed dominant scales ($U \sim 30$ cm/s, $L \sim 30$ km and $f \sim 10^{-4}\ s^{-1}$) leads to values of about 0.1 for the Rossby number.

A related consequence, however, is that a wave with a length of about 50 km with periods of the order of 5–10 days has a phase speed of the order of 10–5 km/day, and therefore the synopticity assumed for the set of CTD profiles has to be questioned. Actually, a phase speed of 10 km/day is of the same order as the sam-

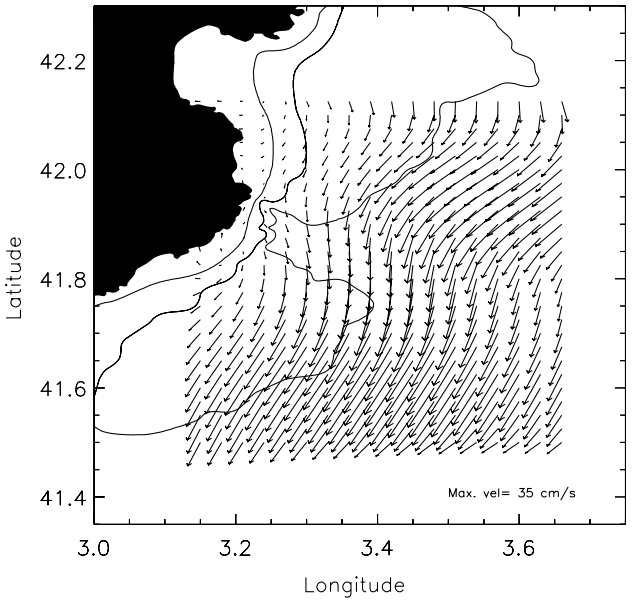

Fig. 12. VM-ADCP velocity at 100 m. Units are cm/s.

pling speed (it took eight days to sample 80 km in the alongshore direction). If these numbers were right, the fact that the sampling was performed from south to north, against the propagation of the meanders, would result in a compression of the wave. That is, the actual gradients (and therefore the inferred vertical velocities) could be significantly smaller than those previously reported. In any case, an upstream sampling is always preferred to a downstream sampling, because in the presence of significant downstream propagation the latter could result in the effective sampling of a very small region, whereas the sampling derived from an upstream survey will effectively cover a wider domain (see Pascual, Gomis, Haney, & Ruiz, 2004 for more details).

3.3. Suspended sediment and downward particulate fluxes

Vertical profiles of suspended sediment concentration in the CTD stations showed values higher than 0.4–0.5 mg l^{-1} along the canyon axis until about 1200 m depth (Fig. 13). Near the bottom, suspended sediment concentration increased reaching maximum values between 500 and 1200 m depth. There were no well defined intermediate turbid layers. Seaward from about 1200 m depth, suspended matter concentration decreased below 0.3 mg l^{-1}. Across the canyon, suspended sediment distribution in the water column was asymmetric showing local turbidity increases near the bottom on the northern and southern walls.

The time series of near-bottom downward particle fluxes and suspended sediment concentrations at the canyon mooring sites are shown in Fig. 14. Along the canyon axis, near-bottom downward total mass fluxes (TMF) were high, both at 470 and 1200 m depth (M2 and M3); the higher ones were not recorded at the 470 m site (mean flux: 28.8 g m^{-2} day^{-1}), but at the 1200 m site (mean flux: 44.3 g m^{-2} day^{-1}). Seaward in the canyon axis at 1700 m depth (M5), total mass fluxes were lower (mean flux: 8.5 g m^{-2} day^{-1}). Total mass fluxes decreased drastically down-canyon from the M3 mooring site. Near-bottom total mass fluxes at the 1700 m depth site on the canyon axis and at the 1200 m depth sites on the canyon walls were from 3 times to one order of magnitude lower than those at the 470 and 1200 m depth sites on the canyon axis. These two sites are closer to the coast and within the canyon part incised in the continental shelf (Fig. 1). On the canyon walls at the 1200 m depth sites (M4 and M6), near-bottom downward particle fluxes were

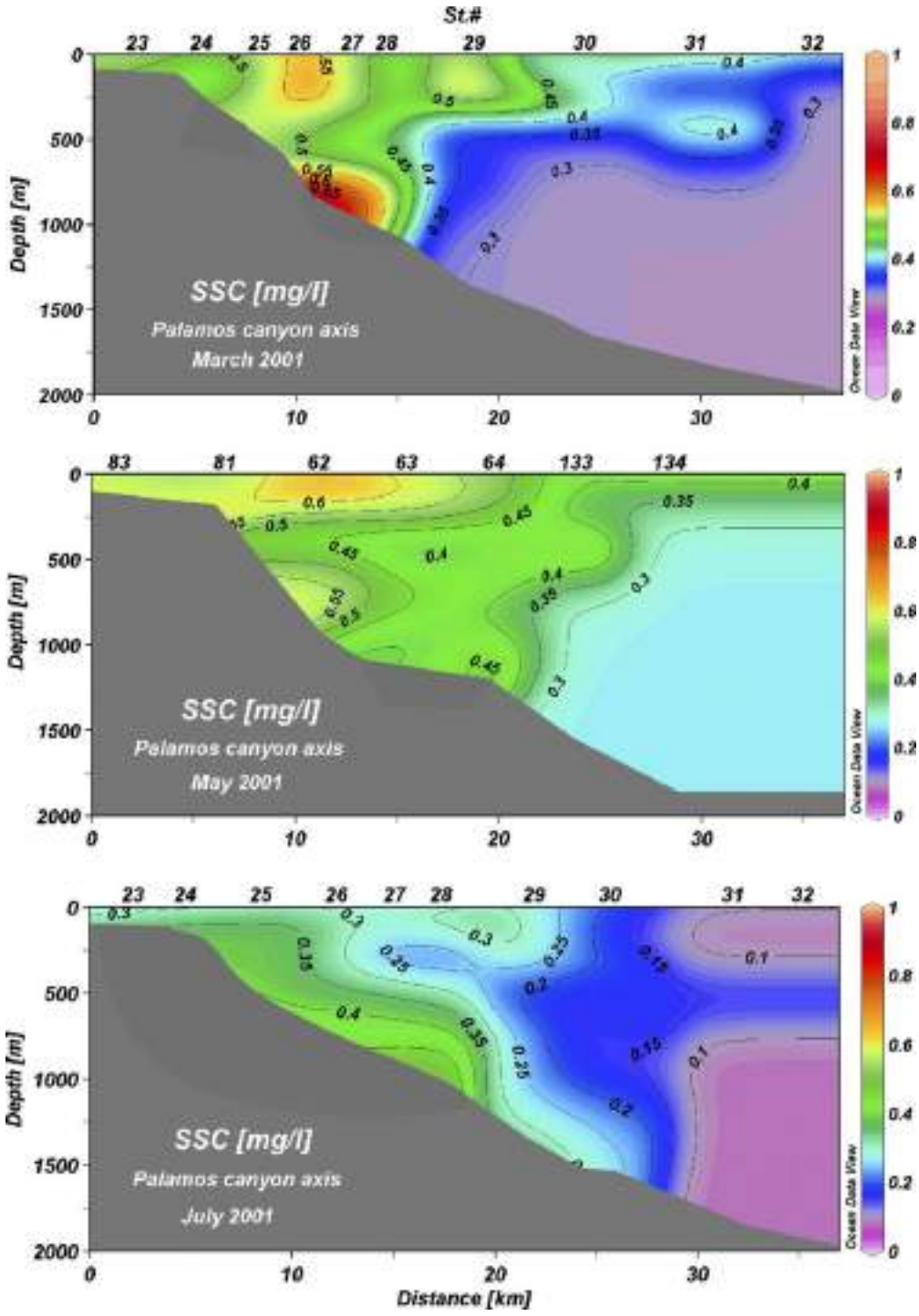

Fig. 13. Cross-margin section along the Palamós canyon axis (location of stations in Fig. 3) showing the distribution of suspended sediment concentration (SSC) during the CANYONS I (March 2001), CANYONS II (May 2001), and CANYONS III (July 2001) cruises.

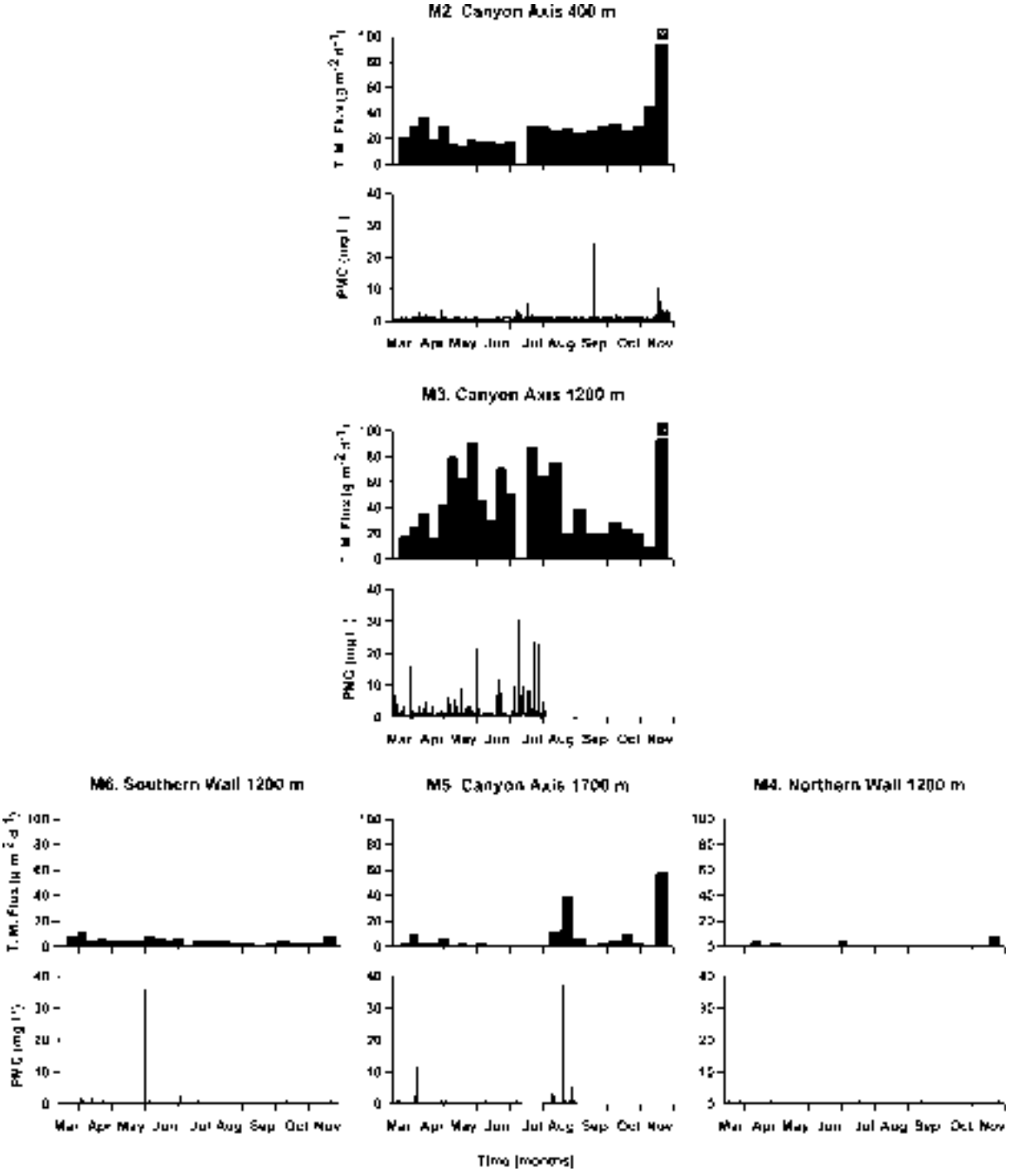

Fig. 14. Temporal series of near-bottom downward particle fluxes and water turbidity (PMC: particulate matter concentration) in the sites of the moorings deployed along the canyon axis at 400, 1200 and 1700 m water depth and in the canyon walls at 1200 m water depth (location in Fig. 1).

more than three times higher on the southern wall (mean flux: 5.1 g m^{-2} day^{-1}) than on the northern wall (mean flux: 1.5 g m^{-2} day^{-1}) (Fig. 14). On the adjacent slope at 1200 m depth (M7), downward particle fluxes (mean flux 0.4 g m^{-2} day^{-1}) were from three times to two orders of magnitude lower than within the canyon, which indicates the canyon role as preferential conduit of particulate matter.

Major biogenic components of the near-bottom downward particle fluxes also show important differences between the more proximal (M2 and M3) and the more distal (M4, M5 and M6) canyon moorings sites. In the canyon axis at the 470 and 1200 m depth sites, the organic C and opal contents were relatively constant being around 1% and 2% respectively. However, seaward in the canyon axis at the 1700 m depth site and on the canyon walls sites, organic C and opal contents increased and were more variable ranging between 1% and 4% and between 2% and 10% respectively.

On the canyon axis, near-bottom turbidity time series at 470 and 1200 m depth showed suspended matter concentrations ranging between 0.4 and 1.4 mg l^{-1} during most of the time, whereas at 1700 m depth, near-bottom turbidity ranged mainly from 0.1 to 0.8 mg l^{-1} during most of the recording period. At these three sites, the time series show spikes corresponding to high turbidity events reaching values of up to 40 mg l^{-1}, lasting between 1 and 6 h (Fig. 14). These turbidity spikes were more frequent in the canyon axis at 1200 m depth and were associated with peaks in the current speed and with significant increases of downward particle fluxes. On the canyon walls at the 1200 m depth sites, suspended sediment concentrations ranged between 0.1 and 1 mg l^{-1} in the southern wall during most of the time (except during some short high-turbidity events) and mainly between 0.1 and 0.6 mg l^{-1} in the northern wall.

Both, near-bottom turbidity and downward particle fluxes were higher in the southern wall than in the northern wall. In fact, near-bottom downward particle fluxes and suspended sediment concentrations on the southern canyon wall were relatively similar to those of the canyon axis at 1700 m (M5) except in a few sampling periods, indicating a stronger influence of the canyon particulate matter on this wall.

A remarkable feature is the sharp increase in downward particle fluxes that occurred in mid-November when a severe storm took place. In the canyon axis, the last cups of the near-bottom sediment traps at 400 m and 1200 m depth overfilled during that event, and a lower but still significant flux increase occurred also in the canyon axis at 1700 m depth and on the canyon walls at 1200 m depth (Fig. 14). This increase was higher on the southern wall than on the northern wall, indicating that during severe storms, the increase of downward particle fluxes affects all the canyon system.

3.4. Seston biomass. Chlorophyll, particulate C and N distribution

Chlorophyll distribution during the March, May and November cruises showed relatively high concentrations decreasing gradually from 1 mg l^{-1} in surface waters to 0.2 mg l^{-1} at about 400 m depth in the canyon area shallower than about 1200 m depth (Fig. 15), whereas in the surrounding area outside the canyon, chlorophyll concentrations higher than 0.2 mg l^{-1} were shallower than 200 m water depth. In addition, in the canyon axis, chlorophyll values of 0.2 μg l^{-1} were often observed locally at depths of about 1000–1200 m. Thus, in the canyon zone up to about 1200 m depth, chlorophyll concentrations were relatively high in intermediate (up to 400 m depth) and locally in near-bottom waters. Seaward, near-bottom chlorophyll values were lower and more similar to those from the open slope. Across the canyon, the distribution of the chlorophyll concentration showed an asymmetric pattern, often with higher values in the southern wall (Fig. 15). This pattern was mostly observed at the head of the canyon and for the cruises of March, July and November.

The particulate carbon (TPC) concentration in surface waters of the Palamós canyon showed values ranging between 70 and 150 μg l^{-1} at most stations and mean values of around 120 μg l^{-1} during the March, July and November cruises. Exceptionally, TPC concentrations of about 260 μg l^{-1} were recorded at some stations of the southern wall during the November cruise. Near the bottom, TPC concentrations were lower and more variable, ranging mainly between 24 and 130 μg l^{-1} and showing mean values of

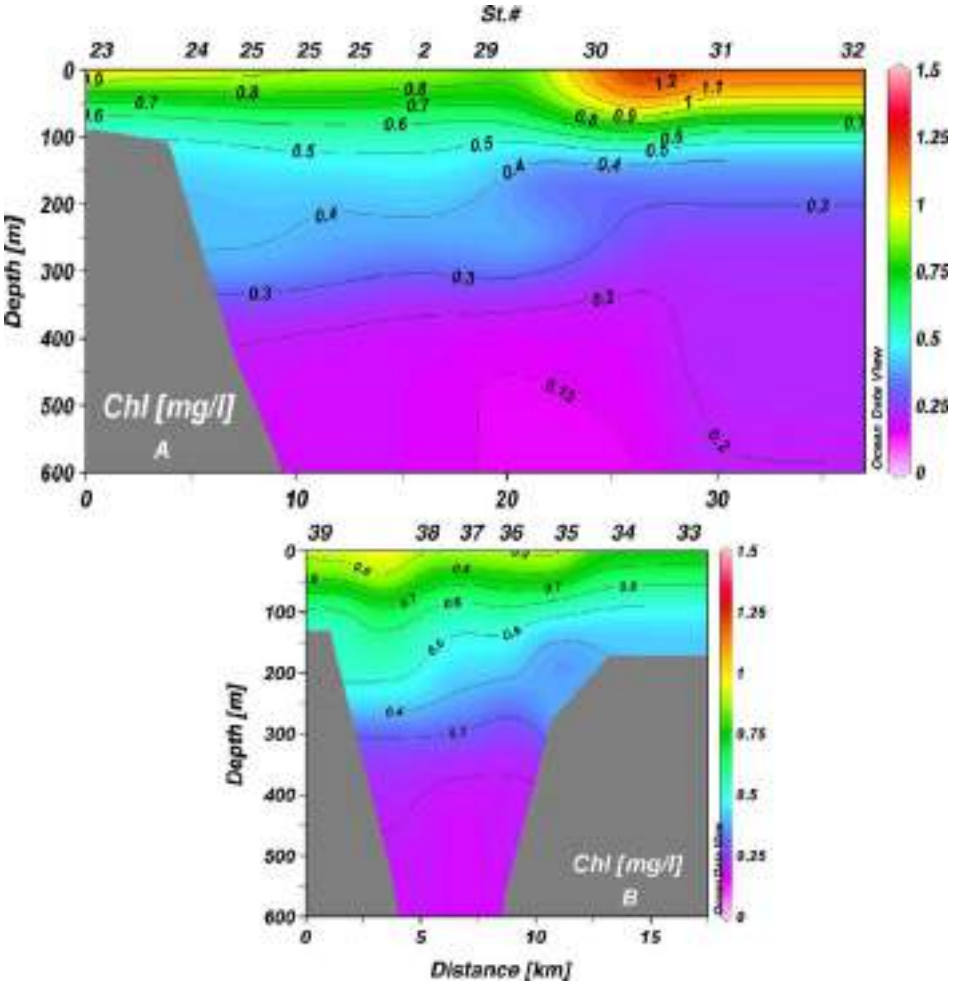

Fig. 15. Cross-margin section along the Palamós canyon axis (location of stations in Fig. 3) showing chlorophyll (Chl) distribution in the upper part of the canyon (A). Across-canyon section (location of stations in Fig. 3) showing chlorophyll (Chl) distribution in the upper part of the canyon (B). Both correspond to CANYONS I (March 2001) cruise.

around 90 $\mu g\, l^{-1}$ inside the canyon. Locally, TPC concentrations of about 260 $\mu g\, l^{-1}$ were recorded at 800 m depth in the canyon axis during the November cruise. Similar trends were also observed for the particulate nitrogen (TPN) distribution. TPN concentrations in surface waters ranged mainly between 7 and 22 $\mu g\, l^{-1}$, with a mean value of about 14 $\mu g\, l^{-1}$. In near-bottom waters, TPN content ranged between 2 and 24 $\mu g\, l^{-1}$ with a mean value of about 8 $\mu g\, l^{-1}$. It is important to point out that both near-bottom TPC and TPN concentrations along the canyon axis were higher in the canyon section up to about 1200 m depth than seaward from this depth (Fig. 16). In addition, TPC and TPN concentrations showed asymmetric distributions often with higher values on the southern canyon wall than on the northern one.

3.5. Ecology and speciation of benthopelagic fauna

In submarine canyons, near-bottom sediment traps can retain organisms that can not be caught with classical methods for plankton studies. Swimmers collected in the Palamós canyon by the near-bottom

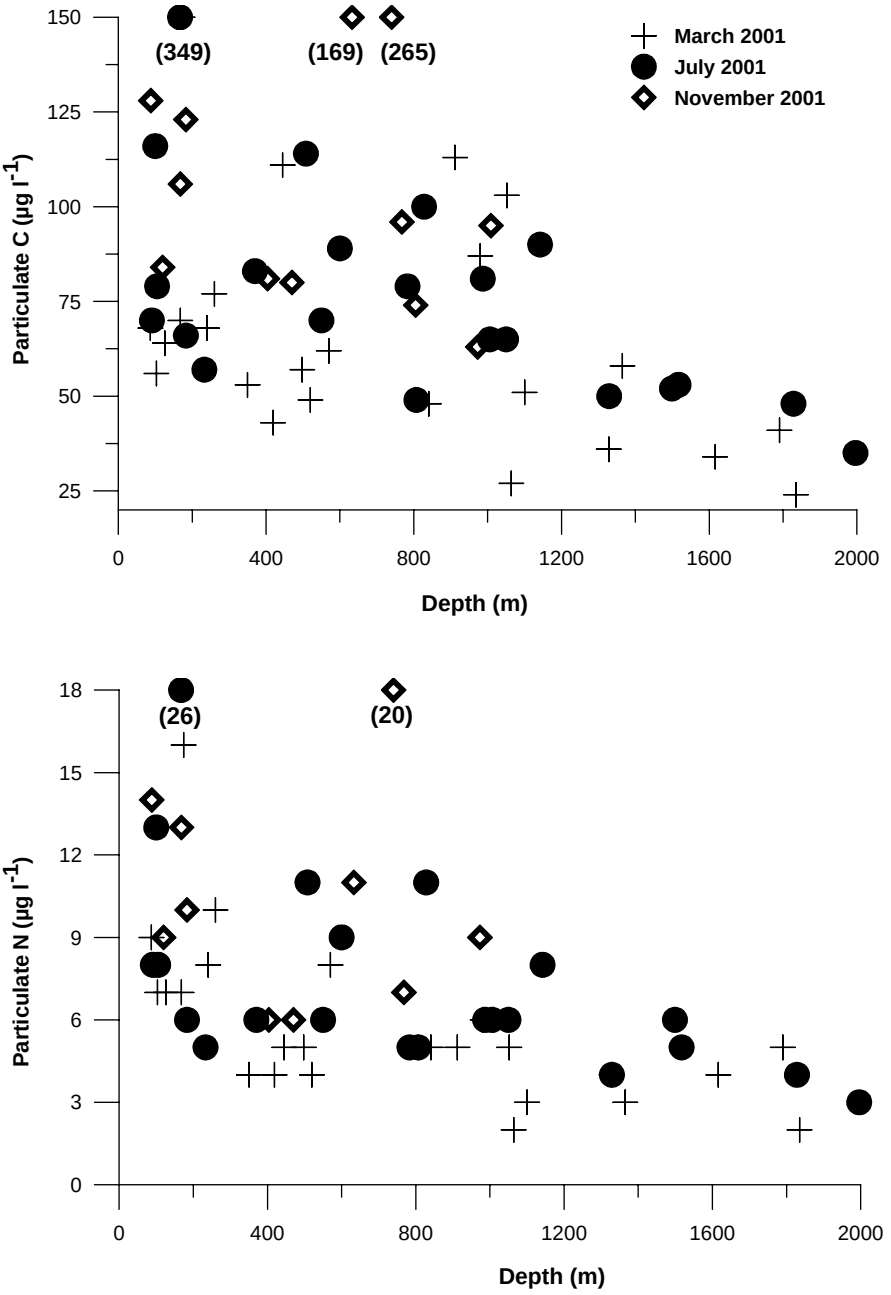

Fig. 16. Graph showing near-bottom particulate carbon and nitrogen concentrations in the canyon. See the lower values seaward from about 1200 m depth.

sediment traps show the high presence of a not yet described benthopelagic species of small elapsipod holothurian that occurs instead of gelatinous zooplankton frequently observed in other studied northwestern Mediterranean canyons (Gili et al., 2000). This holothurian was present only in the deeper traps located near the bottom inside the canyon.

Within the canyon, there are two different main patterns. In the traps located near the canyon head, where the morphology is more constricted (M2 and M3), the fauna is more diverse and the pelagic species dominate. In these traps, polychaetes, copepods, salps and hyperid amphipods together with the medusa *Solmissus albescens* are the most frequent groups. However, in the deeper near-bottom sediment traps an elasipod of small holoturian is dominant and the polychaetes and the specimens of the pelagic mollusc genus *Cavolinia* are also frequent, whereas jellyfish are scarce.

4. Discussion

4.1. On the time variability of the circulation

The observations of the time series of current meters basically show a lack of topographic constraint at upper and intermediate levels, while near the bottom the flow is closely related to the local topography. The averaged currents also suggest a spatial separation of the canyon region closer to the head (shallower than 1200 m depth), sampled by moorings M2 and M3 and the more offshore part of the canyon, sampled by moorings M5 to M8. At M3 in particular, currents at 150 m depth show a significant contribution in the direction opposite to the mean flow and currents at 470 m depth show a rather uniform distribution compared with other sites (with no south-westwards predominant direction and with some clear peaks along the canyon axis). This suggests that a closed circulation can take place in this region, separated from the offshore part of the canyon. A similar pattern has also been deduced from field experiments in similar canyon configurations (i.e., the Blanes canyon, reported by Granata, Vidondo, Duarte, Satta, & García, 1999) and through numerical modelling (Ardhuin et al., 1999).

As stated above, the spectral analysis revealed a low frequency peak around 3 days. Though satellite images, field cruises and time series show the Northern current to have low frequency fluctuations of 3–6 days period associated with meandering or instabilities of the current (i.e., Albérola, Millot, & Font, 1995; Crèpon, Wald, & Monget, 1981; Sammari et al., 1995), it is worth noting that the referred peak is obtained at all depths and with a marked barotropic character. Hence, our hypothesis is that the peak centred at 3 days could be due to trapped topographic waves propagating along the shelf-slope. To investigate this hypothesis we used a linear inviscid model for long coastal-trapped waves propagating on a horizontally uniform stratified ocean with variable topography in the offshore direction (Chapman, 1987). In particular we analysed the contribution of the fundamental mode to the observed variance in longshore velocity in the energetic frequency band of 2–4 days. The equations of motion obtained under these conditions were solved by means of a numerical wave model developed by Brink (1982), which is based on resonance iteration for the frequency at a given wave number and for a range of frequencies smaller than the inertial frequency. In order to prevent a scattering of the energy of low mode coastal trapped waves into higher modes produced by an abrupt change in bottom topography (Hickey, 1995), we calculated the free wave response in a cross-shore segment located upstream of Palamós canyon (mooring M7). We used 55 points in the horizontal and 50 levels in the vertical. The density field was horizontally averaged at depth increments of 10 m down to a depth of 500 m from CTD profiles of CANYONS II, and an exponential fit for the squared Brunt-Väisälä frequency was assumed from 500 m to the bottom. The density profile is illustrated in Fig. 17A.

The theoretical dispersion curve for a coastal trapped wave upstream of Palamós canyon is shown in Fig. 17B. The computed frequencies are represented by circles. The phase speed is nearly constant (36 cm s^{-1}), as shown by the very slight curvature of the dashed line connecting the points. The first point corresponding to the wave number 1×10^{-5} m^{-1} (along-shelf scale of 100 km) has a period of 76 h, which is in agreement with the 3-day period observed for the current variability in the Palamós canyon. This mode is expected to dominate the response because the shelf is relatively narrow and the latitude relatively high (Battisti &

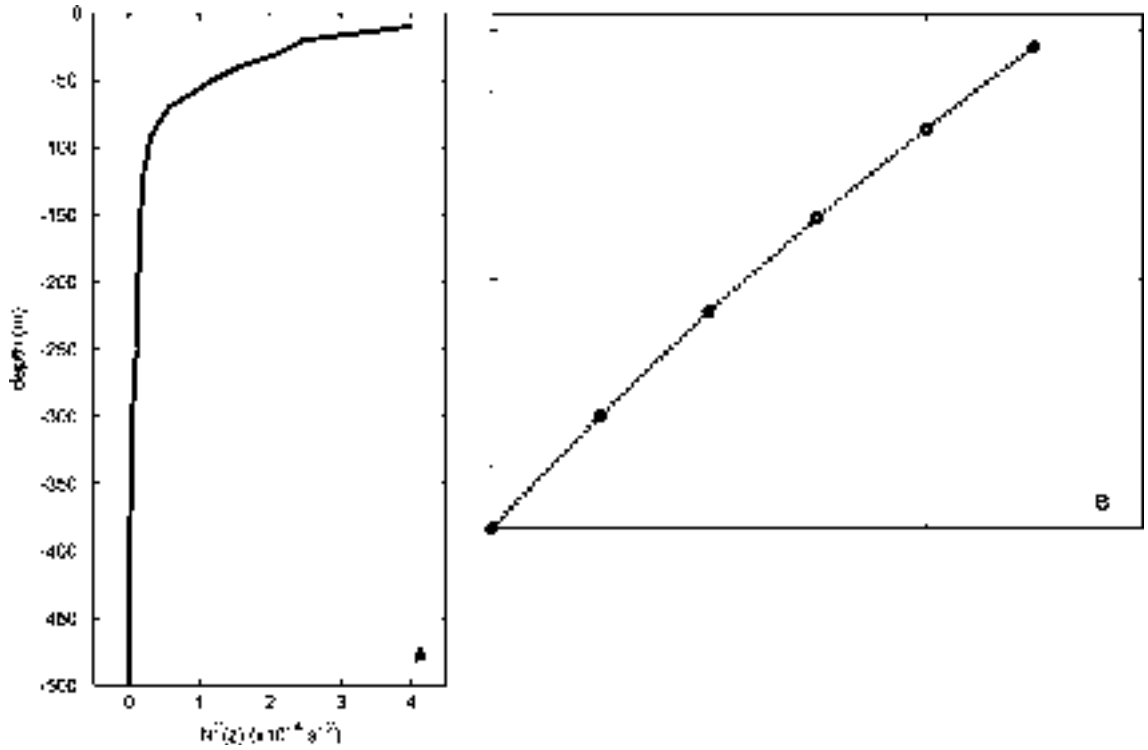

Fig. 17. (A) Topography and stratification profile for computing coastal trapped waves. (B) Dispersion curve for the first coastal-trapped wave mode.

Hickey, 1984). Therefore, this hypothesis must deserve further attention and is being considered in our present research. Although coastal trapped waves have not been reported in the Gulf of Lions and along the Catalan continental margin, several previous studies related to the flow variability seem to indicate the presence of waves propagating along the coast with periods of around 2–4 and 7–10 days (Durrieu de Madron, Radakovitch, Heussner, Loye-Pilot, & Monaco, 1999; Font et al., 1995; Puig et al., 2000).

4.2. On the quasi-synoptic 3D structure of the circulation during the CANYON II cruise

The most remarkable feature is that upper and intermediate layers do not appear to be significantly affected by the presence of the canyon, specially over the offshore half of the canyon. In these layers the distributions of current directions are clearly dominated by the mean south-westwards flow. These results, together with the shift of the observed vertical velocity from that predicted by theoretical and numerical results (downwelling/upwelling should take place on the upstream (northern)/downstream (southern) wall; Klinck, 1996; Skliris, Goffart, Hecq, & Djenidi, 2001), suggest that the meandering of the shelf-edge front observed during the CANYONS II cruise is not due to the presence of the canyon, but to some kind of dynamical instability of the front. In principle, the mean canyon width (about 20 km) and the internal Rossby radius of the incident flow ($R = Ndlf$, with $N = 6 \times 10^{-3}\ s^{-1}$, $d = 300$ m, $f = 10^{-4}\ s^{-1}$) are of the same order, which would allow the canyon to distort the flow (Alvarez et al., 1996). However, the stratification, the other key parameter, is quite strong in the region, with values ranging from a buoyancy frequency of $16 \times 10^{-3}\ s^{-1}$ at upper levels to $2 \times 10^{-3}\ s^{-1}$ at lower (300 m depth) levels. A companion

paper (Jordi, Basterretxea, Orfila, & Tintoré, 2004, this issue) shows via numerical simulation that an upper-level jet flowing over the Palamós canyon can be significantly deflected. However, in these simulations the water column below the jet is almost non-stratified, thus allowing a significant vertical spreading of topographic effects. Instead, for stratification values similar to those observed in the region, several numerical model tests have suggested that the influence of the canyon would not be significant at upper levels (Ardhuin et al., 1999; Klinck, 1996; Skliris et al., 2001).

Finally, a non-canyon-induced meandering of the Northern current during the CANYONS II cruise is also supported by satellite imagery (Fig. 9). Although it cannot be conclusive due to the presence of other canyons upstream of the sampled one, the meandering of the Northern current has often been reported. In particular, Sammari et al. (1995) estimated the wavelength and the period of the meanders as 30–60 km and 3–6 days respectively.

4.3. On suspended sediment and particle fluxes

In the Palamós canyon, near-bottom downward particulate fluxes and suspended matter concentration are relatively high in the canyon axis zone shallower than about 1200 m depth. Offshore from this zone near-bottom particle concentration and fluxes decrease drastically. This suggests the existence of two domains along the canyon axis: the first, landward from about 1200 m depth, with "high" particulate matter load; the second, offshore from this depth, with "low" particulate matter load. The high particulate load zone corresponds to the region where the canyon is incised in the continental shelf and where the circulation is more constricted and closed by the canyon morphology. The low particulate load area is where the canyon incises the continental slope, the morphology is less restricting and the circulation is more closely related to the main flow and the frontal meandering.

The pattern of the sediment fluxes in the Palamós canyon is different from those observed in other Mediterranean canyons, first because of the large downward sediment fluxes and second because it shows higher fluxes in the canyon axis at 1200 m depth than at the canyon head. Downward particle fluxes near the canyon head are from 1.7 to 9 times higher in the Palamós canyon than in other Mediterranean canyons (Heussner, Calafat, & Palanques, 1996; Puig & Palanques, 1998a), but this relation increases drastically at 1200 m depth, where near-bottom particle fluxes of the Palamós canyon are from one to two orders of magnitude higher than in other surrounding canyons.

One particular observation in the Palamós canyon shows the fast (lasting from 1 to 6 h) near-bottom high-turbidity events with increasing current speeds and particle fluxes. These events were mainly recorded at 1200 m depth and were associated with sediment gravity flows triggered by the re-suspension effect of trawling activities in the canyon walls over the mooring site (Palanques et al., 2005). This had not been recorded in any other submarine canyon before. However, although these events often increase particle fluxes in the canyon axis at 1200 m depth, data recorded during periods less influenced by this activity indicate that mean natural fluxes in the Palamós canyon can be around 20 g m^{-2} day^{-1}, which is still about one order of magnitude higher than in other Mediterranean canyons.

Both the high sediment fluxes and the described unusual pattern are related to the fact that the Palamós canyon is more deeply incised in the continental shelf than other studied submarine canyons. In such a scenario, the entrance of particulate matter supplies from the shelf is not restricted to the canyon head (located on the mid-shelf very near the coast) but can also take place through and from the canyon walls incised across the mid- and outer shelf. Particulate matter advected along the shelf can be captured by the canyon circulation when passing over the canyon and sink along with primary produced particles. This is probably why the domain with high particulate load corresponds to the canyon zone incised in the continental shelf. In addition, sediment re-suspended in the shelf and the canyon walls also contribute to increase the particle fluxes. The presence of polychaeta and other benthic fauna in the sediment trap samples along the canyon axis indicate lateral transport of sediment re-suspended in shallower areas.

A clear asymmetry between the canyons walls at about 1200 m depth is observed in the Palamós canyon. On the northern wall, the instantaneous currents are higher and the spectra of bottom current show higher energy than on the southern wall. Downward particle fluxes and suspended sediment concentration on the southern wall are similar to those on the canyon axis at 1700 m depth (the closer mooring site at the canyon axis) and are significantly higher than those recorded on the northern wall, indicating that the southern wall receives higher particulate matter inputs from the canyon than the northern wall. Chlorophyll, TPC and TPN concentrations in the water column near the bottom tend also to be higher on the southern wall than on the northern wall. To explain this asymmetry two hypotheses can be postulated: (1) The existence of an upward water supply on the southern canyon wall; there is no direct evidence for this, but it would be in agreement with the circulation scheme associated with this canyon configuration and observed in numerical models (Jordi et al., 2004, this issue; Klinck, 1996; Skliris et al., 2001) and also with the increase in chlorophyll, TPC and TPN. (2) The effect of the mean flow interacting with the canyon bathymetry. Near the bottom, this flow enters the canyon from the slope along the northern canyon wall and probably accelerates, favouring particulate matter transport instead of suspended particulate matter retention and particle settling. Instead, the mean flow going out of the canyon probably decelerates due to the friction against the southern canyon wall, favouring particle settling and an increase in the suspended particulate matter concentration. These two hypotheses are not mutually exclusive.

4.4. On seston biomass

The relatively high chlorophyll concentrations in the canyon waters up to 400 m depth (Fig. 15) suggest a direct biological input from the coastal biological productivity into the canyon system. Deeper within the canyon up to about 1000 m depth, there are patches where chlorophyll concentrations are $>0.2\ \mu g\ l^{-1}$, being higher than those recorded on the adjacent open slope at similar depths. On the adjacent slope, chlorophyll values $>0.2\ \mu g\ l^{-1}$ were only recorded at depths shallower than 200 m, which indicates a major input of primary produced matter inside the canyon.

The TPC values observed in surface waters of the Palamós canyon are similar to the values reported in the Mediterranean for the open sea, which range between 96 and $168\ \mu g\ l^{-1}$ in spring according to data from Doval, Pérez, and Berdalet (1999). These values are not very different from those recorded in deep waters inside the canyon at 900–1200 m depth and on the southern wall. The maximum values reported for deep waters in the southern wall are comparable to the values observed at shallow stations near the sea floor and during the high productivity period in the Mediterranean ($284 \pm 175\ \mu g\ l^{-1}$, Rossi, & Gili, unpublished data). The TPN values, both in surface and deep waters, were slightly lower than those reported for the open sea ($19–25\ \mu g\ l^{-1}$) and for shallow areas ($17–25\ \mu g\ l^{-1}$). This suggests that waters at about 1200 m depth in the canyon axis and on the southern wall contain as much TPC and TPN as surface Mediterranean waters during high productivity periods, and that channelling of matter from the continental shelf and slope results in high production levels in the submarine canyon.

4.5. On canyon ecology

The analysis of swimmers from the sediment traps of the Palamós canyon must be included in the context of other northwestern Mediterranean submarine canyons. The study of them revealed high levels of fauna specificity in each canyon. For example, in the Foix, Lacaze-Duthiers, and Planier canyons seven new species of medusae were found (38.8% of the total analysed) (Gili et al., 1998, 1999), which is a high number since medusae are one of the best-known zoological groups in the Mediterranean (Boero & Bouil-

lon, 1993). One of the most relevant aspects observed in these studies is the relationship between the number of species, the number of individuals of endemic species and the ecological features of the submarine canyons. Recent studies show that the number of individuals increased progressively as the total flux of organic matter reaching the interior of the canyons increased (Gili et al., 2000). In addition, narrower canyons might heighten isolation while attenuating hydrodynamic processes, and are thus home to larger numbers of individuals. Furthermore, almost all new species were restricted to each of the canyons, thereby highlighting the canyons' isolation effects. In the Palamós canyon, the dominant species, the elasipod holothurian, has not been found in other canyons or elsewhere in the Mediterranean, thus corroborating that canyon isolation favours particular speciation.

Isolation and speciation in submarine canyons must be investigated in terms of geographic distribution and ecological features in geological times. For instance, some species of the studied Mediterranean canyons have been considered Tethys relics which have common ancestors with Pacific Ocean species (Gili et al., 1999). Moreover, the ecological differences between the canyons are probably responsible for generating the allopatric speciation found there. Recent observations on another group of organisms common in the sediment trap samples of Mediterranean canyons including the Palamós canyon, the polychatetes, showed a similar pattern to that described for medusae (Rafael Sardá, personal communication). The polychaete fauna are characterised by undescribed species of the genus *Prinospio* and *Armandia* together with species such as *Spiophanes kroyeri*, *Laonice cirrata* and *Prinospio ehlersi*, which are benthic non-swimming species and therefore can be transported with the particulate matter during re-suspension events. All these species present a seasonal distribution mainly in the deeper traps located near the floor of the canyon axis, and are more abundant in late spring.

The finding of this new fauna indicates the existence of a singular planktonic community in the studied submarine canyons that is probably maintained and diversified by the combined effect of several environmental factors. Fluctuations in the amount of food reaching the bottom would appear to be one of the main factors responsible for the high diversity of deep-sea fauna (Gray, 1997). The data obtained along with other studies around the world indicate that canyons are channels for the transport of large quantities of organic matter from the coastal region to the deep-sea (Vetter & Dayton, 1998). They are very active systems with high production rates and hence locations capable of attaining high faunal richness. In addition, current reversals, vertical currents and upwelling events in submarine canyons may strongly contribute to the biological production processes in many coastal regions. The data obtained also indicate that canyons may play a very important role in speciation processes affecting the deep-water marine fauna, with the involvement of both ecological and evolutionary mechanisms (Gili et al., 1998, 2000). Thus, the discovery of the singular fauna in the studied canyons is helping to investigate the origin of the Mediterranean deep-sea fauna. However, Mediterranean coastal regions are, in turn, overpopulated and the recipients of heavy environmental impacts that may be channelled through the submarine canyons, so this fauna is threatened and could even disappear entirely before it becomes fully known.

Another important biodiversity component of the canyons is related to the benthic stages of planktonic organisms. The life cycles of many planktonic organisms that inhabit the water column include a resting cyst stage in which they eventually sink to the sea bed (Giangrande, Gerasi, & Belmonte, 1994; Montresor, Zingone, & Sarno, 1998). Samples collected in sediment traps set out in the Foix canyon opposite Barcelona have exhibited extremely high concentrations of planktonic cysts of many different morphotypes. Some of the values are the highest, up to 70,000 items m^{-2} day^{-1}, recorded in the Mediterranean (Della Tommasa, Belmonte, Palanques, Puig, & Boero, 2000). In the Palamós canyon, a high concentration of cysts has also been found in the sediment trap samples. This high diversity suggests that the hydrodynamic pattern in canyons and in neighbouring zones is conducive to accumulation and accordingly that more thorough exploration could uncover an unknown level of biodiversity in this habitat.

5. Concluding remarks

Currents in the upper and intermediate water layers of the study area do not appear to be significantly affected by the presence of the Palamós canyon, specially over the offshore half of the canyon, whereas near the bottom the flow is closely related to the local topography. Coastal trapped waves have been identified in the study area confirming their existence in this continental margin, and they seem to be the mechanism generating the low frequency oscillations (3 days) recorded in the Palamós canyon.

Particulate matter fluxes are higher in the Palamós canyon than in other studied north western Mediterranean canyons and also show different spatial and temporal distributions mainly due to morphological constraint (it is deeply incised in the continental shelf), circulation (a closed circulation can take place in the canyon region closer to the head) and anthropogenic activities (trawling).

The Palamós canyon receives a major input of primary produced matter inside the canyon. Channelling of matter from the continental shelf and slope results in high production levels in the submarine canyon up to about 1200 m depth in the canyon axis and on the southern wall. This allows maintaining faunal richness, being more abundant holoturian, polychaetes and pelagic molluscs. The singularity of the dominant species, the elasipod holothurian, corroborates that canyon isolation favours particular speciation.

The data obtained in the Palamós canyon indicate the existence of two domains that differ in the interaction between water circulation, particle dynamics, seston biomass and ecology. One domain is from the canyon head to about 1200 m depth and corresponds to the zone where the canyon incises the continental shelf. The other domain is the canyon region deeper than about 1200 m depth and is where the canyon incises the continental slope. The differences between the two are: (1) in the first domain water circulation is more closed, with surface currents that reverse the mean flow quite often and near bottom currents constrained by the canyon morphology. In the second domain, water circulation is more influenced by the regional circulation driven by the shelf-slope density front, (2) suspended sediment concentration and downward particle fluxes are higher in the first domain than in the second, (3) chlorophyll, TPC and TPN concentrations in deep water are higher in the first domain than in the second, (4) Organic C and opal concentration of downward particle matter is slightly lower in the first domain than in the second, and (5) in the first domain the fauna is more diverse and the pelagic species dominate, whereas in the second the small holoturian is dominant. Important factors for the existence of these two domains are the canyon morphology and the role of the shelf-slope density front.

The southern wall is more influenced by the particulate matter canyon inputs than the northern wall. The across canyon asymmetry of currents, particulate matter and seston may be due to the existence of an upward water supply on the southern canyon wall and/or the effect of the mean flow interacting with the canyon bathymetry.

Acknowledgements

This work was carried out in the framework of the CANYON project funded by the "Dirección General de Enseñanza Superior e Investigación Científica" (MAR99-1060-CO3-01, 02 and 03). It received also additional support from an INTAS project (INTAS-460) and the EuroSTRATAFORM Project (EVK3-CT-2002-00079, EU 5th F.P.). The authors gratefully thank Agustí Julià, Maribel Lloret and Benjamín Casas for their help during the instrument deployments and retrievals, and the officers and crew of the *R/V Garcia del Cid*, for their help and support during surveys. We also thank the "cofradia de pescadors de Palamós" for their collaboration in indicating more secure locations for the shallower mooring and for their interest in our research.

References

Albérola, C., Millot, C., & Font, J. (1995). On the seasonal and mesoscale variabilities of the Northern Current during the PRIMO-0 experiment in the western Mediterranean Sea. *Oceanologica Acta, 18*(2), 163–192.

Alvarez, A., Tintoré, J., & Sabatés, A. (1996). Flow modification and shelf-slope exchange induced by a submarine canyon off the Northeast Spanish coast. *Journal of Geophysical Research, 101*(C5), 12043–12055.

Ardhuin, F., Pinot, J. M., & Tintoré, J. (1999). Numerical study of the circulation in a steep canyon off the Catalan coast (western Mediterranean). *Journal of Geophysical Research, 104*(C5), 11115–11135.

Battisti, D. S., & Hickey, B. M. (1984). Application of remote wind forced coastal trapped wave theory to the Oregon and Washington coasts. *Journal of Physical Oceanography, 14*, 887–903.

Boero, F., & Bouillon, J. (1993). Zoogeography and life cycle patterns of Mediterranean hydroidomedusae (Cnidaria). *Biological Journal of the Linnean Society, 48*, 239–266.

Boyd, P. W., & Newton, P. P. (1999). Does planktonic community structure determine downward particulate organic carbon flux in different oceanic provinces? *Deep-Sea Research I, 46*, 63–91.

Bratseth, A. M. (1986). Statistical interpolation by means of successive correction. *Tellus, 38A*, 439–447.

Brink, K. H. (1982). A comparison of long coastal trapped wave theory with observations off Peru. *Journal of Physical Oceanography, 12*, 897–913.

Buscail, R., & Germain, C. (1997). Present-day organic matter sedimentation on the NW Mediterranean margin: Importance of off-shelf export. *Limnology and Oceanography, 42*, 217–229.

Cartes, J. E. (1998). Dynamics of the Bathyal Benthic Boundary Layer in the northwestern Mediterranean: Depth and temporal variations in macrofaunal–megafaunal communities and their possible connections within deep-sea trophic webs. *Progress in Oceanography, 41*, 111–139.

Castellón, A., Font, J., & García, E. (1990). The Liguro-Provençal-Catalan current (NW Mediterranean) observed by Doppler profiling in the Balearic Sea. *Scientia Marina, 54*, 269–276.

Chapman, D. C. (1987). Application of wind-forced, long, coastal-trapped wave theory along the California coast. *Journal of Geophysical Research, 92*, 1789–1816.

Crèpon, M., Wald, L., & Monget, J. M. (1981). Low-frequency waves in the Ligurian sea during December 1977. *Journal of Geophysical Research, 87*(C1), 595–600.

Della Tommasa, L., Belmonte, G., Palanques, A., Puig, P., & Boero, F. (2000). Resting stages in a submarine canyon: A component of shallow-deep-seacoupling? *Hydrobiologia, 440*(1–3), 249–260.

Demestre, M., & Martín, P. (1993). Optimum exploitation of a demersal resource in the western Mediterranean: The fishery of the deepwater shrimp *Aristeus antennatus*. *Scientia Marina, 57*, 175–182.

Doval, M. D., Pérez, F. F., & Berdalet, E. (1999). Dissolved and particulate organic carbon and nitrogen in the northwestern Mediterranean. *Deep-Sea Research I, 46*, 511–527.

Drake, D. E., & Gorsline, D. S. (1973). Distribution and transport of suspended particulate matter in Hueneme, Redondo, Newport and La Jolla submarine canyons. *Geological Society of America Bulletin, 84*, 3949–3968.

Durrieu de Madron, X. (1994). Hydrography and nepheloid structures in the Grand-Rhone canyon. *Continental Shelf Research, 14*, 457–477.

Durrieu de Madron, X., Radakovitch, O., Heussner, S., Loye-Pilot, M. D., & Monaco, A. (1999). Role of the climatological and current variability on shelf-slope exchanges of particulate matter: Evidence from the Rhône continental margin (NW Mediterranean). *Deep-Sea Research I, 46*, 1513–1538.

Flexas, M. M., Durrieu de Madron, X., Garcia, M. A., Canals, M., & Arnau, P. (2002). Flow variability in the Gulf of Lions during the MATER HFF experiment (March–May 1997). *Journal of Marine Systems, 33–34*, 197–214.

Font, J., García-Ladona, E., & Górriz, E. G. (1995). The seasonality of mesoscale motion in the Northern Current of the western Mediterranean: Several years of evidence. *Oceanologica Acta, 18*, 207–219.

Font, J., Salat, J., & Tintoré, J. (1988). Permanent features of the circulation in the Catalan Sea. *Oceanologica Acta, 9*, 51–57.

García, E., Tintoré, J., Pinot, J. M., Font, J., & Manríquez, M. (1994). Surface circulation and dynamics of the Balearic Sea. In: P. La Violette, *Seasonal and interannual variability of the western Mediterranean Sea*. American Geophysical Union, *Coastal and Estuarine Studies, 46*, 73–91.

Gardner, W. D. (1989a). Baltimore canyon as a modern conduit of sediment to the deep sea. *Deep-Sea Research, 36*, 323–358.

Gardner, W. D. (1989b). Periodic resuspension in Baltimore canyon by focusing of internal waves. *Journal of Geophysical Research, 94*, 18185–18194.

Giangrande, A., Gerasi, S., & Belmonte, G. (1994). Life-cycle and life-history diversity in marine invertebrates and the implications in community dynamics. *Oceanography and Marine Biology: An Annual Review, 32*, 305–333.

Gili, J. M., Bouillon Pagès, J. F., Palanques, A., & Puig, P. (1999). Submarine canyons as habitat of singular plankton populations: three new deep-sea hydromedusae in the western Mediterranean. *Zoology Journal of the Linnean Society, 125*(3), 313–329.

Gili, J. M., Bouillon, J., Pagès, F., Palanques, A., Puig, P., & Heussner, S. (1998). Origin and biogeography of the deep-water Mediterranean hydromedusae including the description of two new species collected in submarine canyons of northwestern Mediterranean. *Scientia Marina, 62*, 113–134.

Gili, J. M., Bouillon, J., Pagès, F., Palanques, A., Puig, P., Heussner, S., et al. (2000). A multidisciplinary approach to the knowledge of gelatinous zooplankton populations inhabiting Mediterranean submarine canyons. *Deep-Sea Research I, 47*, 1513–1533.

Granata, T. C., Vidondo, B., Duarte, C. M., Satta, M. P., & García, M. (1999). Hydrodynamics and particle transport associated with a submarine canyon off Blanes (Spain, NW Mediterranean Sea). *Continental Shelf Research, 19*, 1249–1263.

Gray, J. S. (1997). Marine biodiversity: Patterns, threats and conservation needs. *Biodiversity and Conservation, 6*, 153–175.

Greene, C. H., Wiebe, P. H., Burczynski, J., & Youngbluth, M. J. (1992). Acoustical detection of high-density demersal krill layers in the submarine canyons off Georges Bank. *Science, 241*, 359–361.

Guillén, J., Palanques, A., Puig, P., Durrieu de Madron, X., & Nyffeler, F. (2000). Field calibration of optical sensors for measuring suspended sediment concentration in the western Mediterranean. *Scientia Marina, 64*(4), 427–435.

Heussner, S., Ratti, C., & Carbonne, J. (1990). The PPS 3 timeseries sediment trap and the trap sample processing techniques used during the ECOMARGE experiment. *Continental Shelf Research, 10*, 943–958.

Heussner, S., Calafat, A. M., & Palanques, A. (1996). Quantitative and qualitative features of particle fluxes in the North-Balearic Basin. In M. Canals, J. L. Casamor, I. Cacho, A. M. Calafat, & A. Monaco (Eds.). *EUROMARGE-NB Final Report MAST II Programme* (Vol. II, pp. 43–66). Brussels: European Union.

Hickey, B. M. (1995). Coastal submarine canyons. In P. Müller & D. Henderson (Eds.), *Topographic effects in the ocean* (pp. 95–110). Manoa: School of Ocean and Earth Science and Technology.

Hickey, B. M. (1997). The response of a steep-sided, narrow canyon to time-variable wind forcing. *Journal of Physical Oceanography, 27*, 697–726.

Hickey, B. M., Baker, E. T., & Kachel, N. (1986). Suspended particle movement in and around Quinault submarine canyon. *Marine Geology, 71*, 35–83.

Hoskins, B. J., Draghici, I., & Davis, H. C. (1978). A new look at the omega-equation. *Quarterly Journal of the Royal Meteorological Society, 104*, 31–38.

Hotchkiss, F. S., & Wunsch, C. (1982). Internal waves in Hudson canyon with possible geological implications. *Deep-Sea Research, 29*, 415–442.

Hunkins, K. (1988). Mean and tidal currents in Baltimore canyon. *Journal of Geophysical Research, 93*, 6917–6929.

Jordi, A., Basterretxea, G., Orfila, A., & Tintoré, J. (2004). Shelf-slope exchanges by frontal variability in a steep submarine canyon. *Progress on Oceanography*, this issue.

Klinck, J. M. (1996). Circulation near submarine canyons: A modelling study. *Journal of Geophysical Research, 101*, 1211–1223.

La Violette, P. E., Tintoré, J., & Font, J. (1990). The surface circulation of the Balearic Sea. *Journal of Geophysical Research, 95*, 1559–1568.

López García, M. J., Millot, C., Font, J., & García-Ladona, E. (1994). Surface circulation variability in the Balearic Basin. *Journal of Geophysical Research, 99*, 3285–3296.

Margalef, R. (1997). Our biosphere. *Excellence in ecology* (Vol. 10, pp. 176). Oldendorf/Luhe: Ecology Institute.

Masó, M., & Tintoré, J. (1991). Variability of the shelf waters off the northeast Spanish coast. *Journal of Marine Systems, 1*, 441–450.

McHugh, C. N., Ryan, W. B. F., & Hecker, B. (1992). Contemporary sedimentary processes in the Monterey canyon-fan system. *Marine Geology, 107*, 35–50.

Millot, C. (1985). Evidence of a several-day propagating wave. *Journal of Physical Oceanography, 15*, 258–272.

Millot, C. (1999). Circulation in the western Mediterranean Sea. *Journal of Marine Systems, 20*, 423–442.

Montresor, M., Zingone, A., & Sarno, D. (1998). Dinoflagellate cyst production at a coastal Mediterranean site. *Journal of Plankton Research, 20*, 2291–2312.

Mortlock, R. A., & Froelich, P. N. (1989). A simple method for the rapid determination of biogenic opal in pelagic sediments. *Deep-Sea Research, 36*, 1415–1426.

Palanques, A., Martín, J., Puig, P., Guillén, J., Company, J. B., Sardá, F., (2005). Effects of sediment gravity flows induced by trawling in the Palamoś (Fonera) submarine canyon (northwestern Mediterranean). *Deep-Sea Research*, in press.

Pascual, A., Gomis, D., Haney, R. L., & Ruiz, S. (2004). A quasi-geostrophic analysis of a meander in the Plamós canyon: Vertical velocity, geopotential tendency and a relocation technique. *Journal of Physical Oceanography, 34*, 2274–2287.

Pedder, M. A. (1993). Interpolation and filtering of spatial observations using successive corrections and gaussian filters. *Monthly Weather Review, 121*, 2889–2902.

Pinot, J. M., Tintoré, J., & Gomis, D. (1995). Multivariate analysis of the surface circulation in the Balearic Sea. *Progress in Oceanography, 36*, 343–376.

Pinot, J. M., Tintoré, J., & Wang, D. P. (1996). A study of the omega equation for diagnosing vertical motions at ocean fronts. *Journal of Marine Research, 54*, 239–259.

Puig, P., & Palanques, A. (1998a). Nepheloid structure and hydrographic control on the Barcelona continental margin, north-western Mediterranean. *Marine Geology, 149*, 39–54.

Puig, P., & Palanques, A. (1998b). Temporal variability and composition of settling particle fluxes on the Barcelona continental margin (north-western Mediterranean). *Journal of Marine Research, 56*, 639–654.

Puig, P., Palanques, A., Guillén, J., & García-Ladona, E. (2000). Deep slope currents and suspended particle fluxes in and around the Foix submarine canyon (NW Mediterranean). *Deep-Sea Research, 47*, 343–366.

Rossi, S., & Gili, J. M. (unpublished data). Composition and temporal variation of the near-bottom seston in a Mediterranean coastal area. *Marine Biology*.

Sammari, C., Millot, C., & Prieur, L. (1995). Aspects of the seasonal and mesoscale variabilities of the northern current in the western Mediterranean Sea inferred from the PROLIG-2 and PROS-6 experiments. *Deep-Sea Research I, 42*(6), 893–917.

Schlitzer, R., Ocean Data View, http://www.awi-bremerhaven.de/GEO/ODV, 2003.

Shepard, F. P., Marshall, N. F., McLoughlin, P. A., & Sullivan, G. G. (1979). *Currents in submarine canyons and other seavalleys* (173 pp.). Tulsa: The American Association of Petroleum Geologists.

Skliris, N., Goffart, A., Hecq, J. H., & Djenidi, S. (2001). Shelf-slope exchanges associated with a steep submarine canyon off Calvi (Corsica, NW Mediterranean Sea): A modelling approach. *Journal of Geophysical Research, 106*(C9), 19883–19901.

Stefanescu, C., Morales-Nin, B., & Massutí, E. (1994). Fish assemblages on the slope in the Catalan Sea (western Mediterranean): Influence of a submarine canyon. *Journal of the Marine Biological Association of the United Kingdom, 74*, 499–512.

Thunell, R. C. (1998). Particle fluxes in a coastal upwelling zone: Sediment trap results from Santa Barbara Basin, California. *Deep-Sea Research II, 45*, 1863–1884.

Tintoré, J., Wang, D. P., & La Violette, P. E. (1990). Eddies and thermohaline intrusions of the shelf-slope front off the northeast Spanish coast. *Journal of Geophysical Research, 95*, 1627–1633.

Vetter, E. W. (1994). Hotspots of benthic production. *Nature, 372*, 47.

Vetter, E. W. (1995). Detritus-based patches of high secondary production in the nearshore benthos. *Marine Ecology Progress Series, 120*, 251–262.

Vetter, E. W., & Dayton, P. K. (1998). Macrofaunal communities within and adjacent to a detritus-rich submarine canyon system. *Deep-Sea Research I, 11*, 25–54.

Wang, D. P., Vieira, M. E. C., Salat, J., Tintoré, J., & La Violette, P. E. (1988). A shelf-slope filament off the Northeast Spanish coast. *Journal of Marine Research, 46*, 321–332.

Yentsch, C. S., & Menzel, D. W. (1963). A method for the determination of phytoplankton chlorophyll and phaeophytin by fluorescence. *Deep-Sea Research, 10*, 221–231.